II.E. Vitreoretinal Interface and Inner Limiting Membrane

Chapter · September 2014

DOI: 10.1007/978-1-4939-1086-1_11

CITATIONS
20

READS
1,065

3 authors, including:

Willi Halfter
University of Pittsburgh
132 PUBLICATIONS **5,976** CITATIONS

SEE PROFILE

Jerry Sebag
VMR Institute for Vitreous Macula Retina
205 PUBLICATIONS **5,678** CITATIONS

SEE PROFILE

Vitreoretinal Interface and Inner Limiting Membrane

II.E.

Willi Halfter, J. Sebag, and Emmett T. Cunningham Jr.

Outline

Keywords
Vitreous • Vitreoretinal interface • Inner limiting membrane • Extracellular matrix • Biochemistry Ultrastructure • Development • Aging • Disease

Key Concepts

1. The vitreoretinal interface has three components: the inner limiting membrane, the posterior vitreous cortex, and an intervening extracellular matrix responsible for vitreoretinal adhesion.
2. Aging and disease alter the vitreoretinal interface and play an important role in tractional as well as proliferative disorders at the vitreoretinal interface.
3. The vitreoretinal interface influences oxygenation, nutrition, drug delivery, and viral penetration as vectors for future retinal therapeutics.

W. Halfter, PhD
Department of Neurobiology, University of Pittsburgh,
200 Lothrop Street STE W1415, Pittsburgh, PA 15261, USA
e-mail: whalfter@pitt.edu

J. Sebag, MD, FACS, FRCOphth, FARVO (✉)
VMR Institute for Vitreous Macula Retina,
7677 Center avenue, Huntington Beach, CA 92647, USA

Doheny Eye Institute, Los Angeles, CA, USA
e-mail: jsebag@VMRinstitute.com

E.T. Cunningham Jr., MD, PhD, MPH
The Uveitis Service, West Coast Retina Medical Group,
Department of Ophthalmology, California Pacific Medical Center,
Stanford University School of Medicine,
2340 Clay Street, Fifth Floor, San Francisco, CA 94115, USA
e-mail: emmett_cunningham@yahoo.com

I. Introduction

The vitreoretinal interface is the site of many pathogenic events associated with sequences that lead to vision loss. The interface consists of a complex formed by the inner limiting

J. Sebag (ed.), *Vitreous: in Health and Disease*,
DOI 10.1007/978-1-4939-1086-1_11, © Springer Science+Business Media New York 2014

Figure II.E-1 Human vitreoretinal interface. At the *top* of the figure, vitreous collagen fibrils are densely packed within a layer known as the posterior vitreous cortex (*PVC*), which overlies the ILM of the retina. Between these two structures is an intervening extracellular matrix (*ECM*), called by Heergaard the "vitreoretinal border region"

lamina of the retina, commonly called the inner limiting membrane (ILM), the posterior vitreous cortex, and an intervening extracellular matrix that is thought to be responsible for vitreoretinal adhesion (Figure II.E-1). Changes in each of these three components occur with aging and in certain diseases, such as myopia and diabetes. These aging and disease-related changes contribute a variety of vitreoretinal disorders. There are special interfaces between vitreous and the optic disc (see chapter III.E. Vitreo-papillary adhesion/traction) and retinal blood vessels, with the latter contributing to various retinovascular disorders (see chapters III.A. Congenital vascular vitreo-retinopathies; III.K. Vitreous in retino-vascular diseases and diabetic macular edema; V.A.6. Vitreous surgery of arterial and venous retino-vascular diseases)

II. Inner Limiting Membrane

For years there was disagreement regarding the existence of an inner limiting membrane (ILM) of the retina. Some believed that the limiting membrane of the vitreous (*membrana hyaloidea*) served as the inner limiting membrane of the retina. Others believed that there was an ILM but that no limiting membrane existed around the vitreous. In 1912, Salzmann proposed a middle ground by stating that *In any case, one must say that this membrane has just as much relation to the vitreous as it has to the retina, and that it looks like the inner glass membrane of the retina in one preparation and like the outer border membrane of the vitreous in another* [1]. In point of fact, both concepts were right. There are

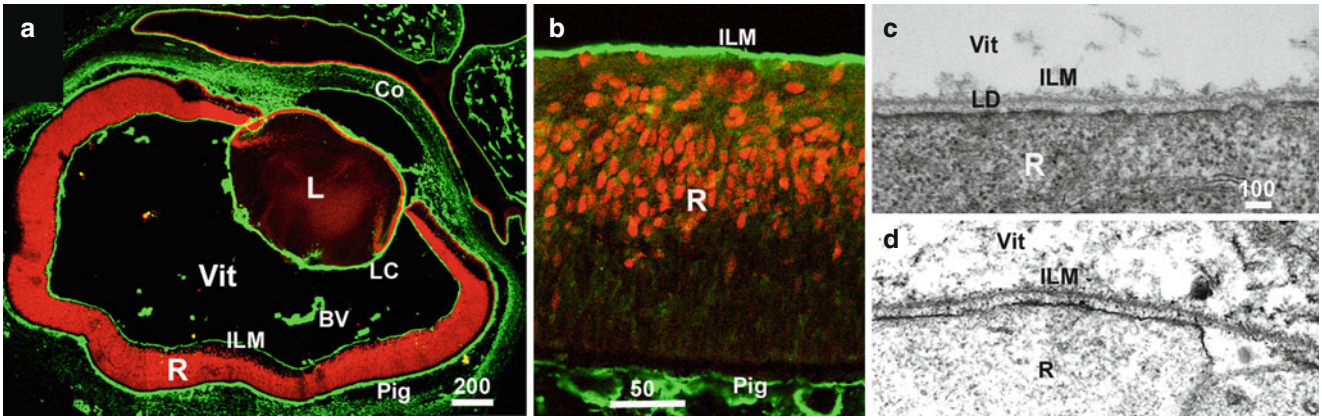

Figure II.E-2 Location and ultrastructure of the fetal human ILM. Fluorescence micrograph showing a cross section of a 10-week-old fetal human eye. (**a**) This section was stained for collagen IV (*green*) and shows the location of the ILM, the vascular BMs of the hyaloid blood vessels (*BV*), the corneal BMs (*Co*), the BMs of the pigment epithelium (*Pig*) in Bruch's membrane, and the lens capsule (*LC*). The section had been counterstained with an antibody to Pax6, a nuclear transcription factor that is present in all ocular cells (*red*). (**b**) A high power view of the fetal human retina stained for agrin, a BM proteoglycan (*green*) shows the ILM and the BM of the pigment epithelium (*Pig*). Counterstaining with Islet 1 shows the location of the differentiated ganglion cells at the vitread side of the retina. (**c**) A TEM micrograph of the vitread surface of the fetal human retina shows that the ILM appears as a thin sheet of ECM at the vitreoretinal border region with a distinctive lamina densa (*LD*). The ultrastructure of the fetal ILM resembles the classic textbook morphology of a typical BM. (**d**) The neonatal mouse ILM is shown for comparison. The mouse ILM is morphologically very similar to the fetal human ILM (compare **c**, **d**). *BM* basement membrane, *ILM* inner limiting membrane, *R* retina, *L* lens (Bars: **a**: 200 μm; **b**: 50 μm; **c**, **d**: 100 nm)

distinct "limiting membranes" demarcating the boundary of both the retina and adjacent vitreous, although neither is a membrane in the classic histological sense of a cell membrane and they are often therefore called "laminae."

The "limiting membrane" of the retina is formed by the contiguous basement membranes of Mueller cells. The "limiting membrane" of the vitreous, in contrast, is formed by the posterior vitreous cortex, a structure composed of densely packed vitreous collagen fibrils [1]. Between the two is an interdigitating extracellular matrix that contains elements of each, described by Heegaard as the "vitreoretinal border region" [2].

A. Anatomy

1. Structure

Despite the fact that the ILM is not a true membrane in the lipid-rich, cell membrane sense, Salzmann [1] preferred the term "membrana limitans interna," primarily because the ILM is a basement membrane (BM) functionally analogous with the BM covering the inner surface of the ciliary epithelium. Embryologically, the ILM shares ontogeny with the pial BM which envelopes the entire central nervous system. In the eye, the ILM is one of six BMs that includes (1) the lens capsule, which is the thickest BM of the body; (2) the hyaloid vascular BMs of the vitreous and the retina; (3) the two corneal BMs; (4) the ILM; (5) the BM of the pigment epithelium; and (6) the BM sub-layer of Bruch's membrane (Figure II.E-2).

The ILM, like all other BMs, is transparent, very thin, and difficult to localize by conventional histology. The ILM can, however, be readily detected by either immunocytochemistry using antibodies specific to BM proteins (Figure II.E-2a, b) or transmission electron microscopy (TEM; Figures II.E-1 and II.E-2c, d). High-resolution TEM of fetal human eyes shows the ILM to be an extracellular matrix sheet with a thickness of less than 100 nm. The fetal human ILM can be subdivided into an outer lamina lucida layer that faces the ECM of the vitreoretinal border region, a central electron-dense lamina densa, and a second inner lamina lucida that faces the end feet of the retinal Müller glial cells [2].

The thickness and morphology of the fetal human ILM resembles the ultrastructure of the classical textbook BMs. Heegaard described that the human ILM increases markedly in thickness during the first months/years of life in the equatorial and macular regions. The thickness is stable from the second decade and remains unchanged throughout subsequent decades. In all human adult eyes that were studied, the ILM was the thickest in the macular region [2].

This information may not be accurate, however, as TEM, which is traditionally used to determine the thickness of BMs and the ILM, may be fraught with artifacts. Since TEM requires chemical fixation and dehydration of tissues, this may result in distortion and artifacts. Recently, Atomic force microscopy (AFM) has been introduced to examine the morphology and biomechanical properties of isolated and flat-mounted BMs [3, 4], including measurements of ILM thickness. AFM uses a fine tip on the flexible cantilever that

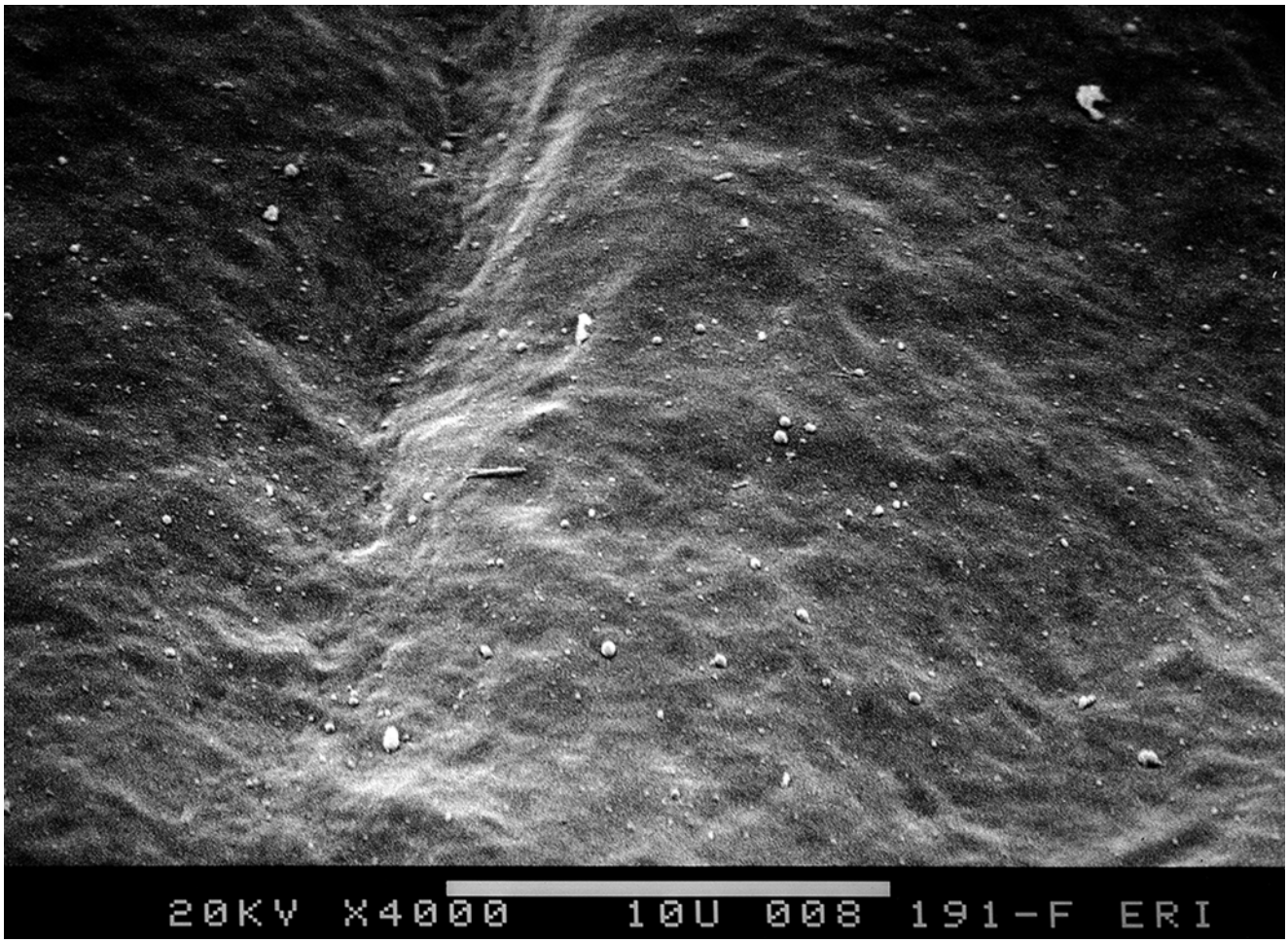

Figure II.E-3 Scanning electron microscopy of the anterior aspect of human ILM, after peeling the retina off the vitreous postmortem in a human adult. The anterior (vitread) surface of the ILM is smooth: (magnification bar = 10 microns)

scans over the surface of the samples. The degree of cantilever deflection, as recorded by a laser beam, can be used to (a) image the sample at atomic resolution, (b) measure its thickness, and (c) assess its stiffness [5–9]. Since AFM can also scan the samples when they are submerged in PBS, AFM can be used to examine unfixed and fully hydrated BMs.

AFM examination revealed that the thickness of the embryonic chick and adult human ILMs is, under native conditions, between two to four times greater than previously measured by TEM [3, 4]. The fact that AFM-based thickness measurements of dehydrated ILMs are very similar to the thickness data obtained by TEM shows that sample preparation, most importantly, its dehydration, results in a dramatic 50 % shrinkage [3]. An independent study measuring lens capsule thickness by confocal microscopy, also under native conditions, showed that hydrated lens capsules are at least twice thicker than previously determined by TEM [10]. Thus, sample preparation for TEM introduces massive shrinkage and possibly a distortion of BM morphology.

The massive shrinkage of the ILM after dehydration is due to the loss of water that is tightly bound by the glycosaminoglycans of proteoglycans that are abundantly present in BMs. Proteoglycans are highly glycosylated proteins with glycosaminoglycan side chains that carry a large net negative charge. The high density of negative charge of proteoglycans is responsible for substantial water retention in cartilage [11] and vitreous [12] and indicates a similar function of proteoglycans in the ILM. Experimental confirmation for this concept comes from the ILM thickness and stiffness data after enzymatic removal of the GAG side chains that results in 50 % shrinkage and a doubling of the ILM stiffness [4, 13]. Based on the AFM data, we can infer that about 50 % of the ILM mass is water, tightly bound by proteoglycans, and that water is the most abundant component of the ILM. Further, the hydration status determines the stiffness of the ILM.

2. Topographic Variations

In the entire fundus, the anterior aspect of the ILM has a smooth appearance (Figure II.E-3). However, the posterior aspect of the ILM varies in structure by location: in the periphery (Figure II.E-4b), the posterior aspect of the ILM is smooth and resembles the anterior aspect. However, in the posterior pole (Figure II.E-4a), the posterior aspect of

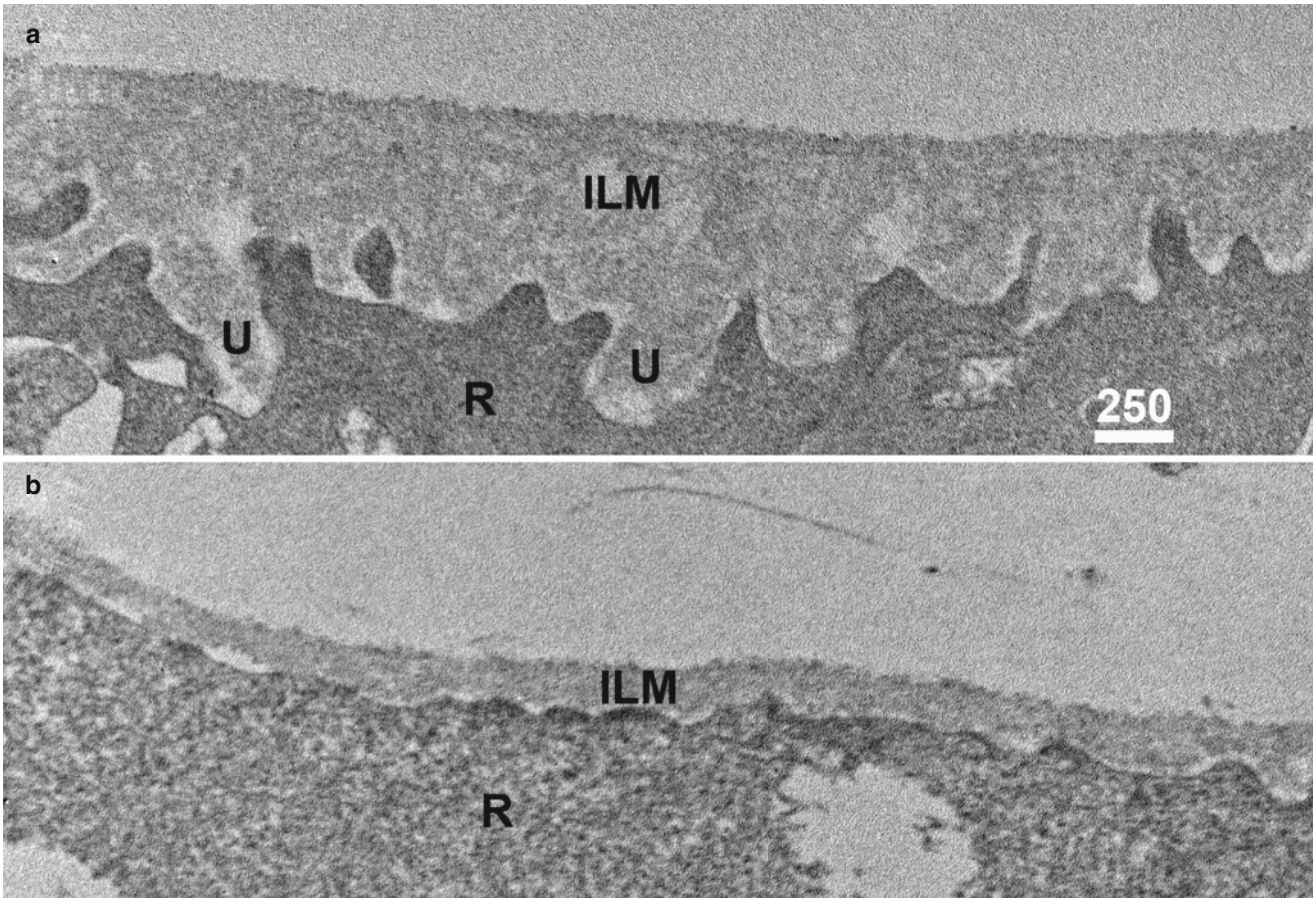

Figure II.E-4 Topographic variation in the human ILM. (**a**) Transmission electron microscopy of the inner limiting membrane (*ILM*) in the posterior pole of a 27-year-old human demonstrating "undulations" (*U*) in the posterior aspect of the ILM that fills the crevices between the underlying retinal (*R*) cells (Bar = 250 nm). (**b**) Transmission electron microscopy of the ILM in the peripheral fundus of the same eye as in (**a**) demonstrates that the posterior aspect of the ILM resembles the anterior aspect of the ILM with a continuous surface and minimal undulations (Bar = 250 nm)

the ILM "undulates" in an irregular configuration filling the crevices between underlying retinal glia and nerve fibers.

At the rim of the optic disc (see chapter III.E. Vitreopapillary adhesion and traction), the retinal ILM ceases, although the basement membrane continues as the "inner limiting membrane of Elschnig" [14]. This membrane is 50 nm thick and is believed to be formed by the basal lamina of the astroglia in the optic nerve head. At the central-most portion of the optic disc, the membrane thins to 20 nm, follows the irregularities of the underlying cells of the optic nerve head, and is composed only of glycosaminoglycans and no collagen [14]. This structure is known as the "central meniscus of Kuhnt." Balazs [12] has stated that the Müller cell basal lamina prevents the passage of cells as well as any molecules larger than 15–20 nm and proposed that the complex of the posterior vitreous cortex and ILM could act as a "molecular sieve." Consequently, the thinness and chemical composition of the central meniscus of Kuhnt and the membrane of Elschnig may account for, among other phenomena, the frequency with which abnormal cell proliferation arises from or near the optic nerve head in proliferative diabetic retinopathy and premacular membrane formation.

The ILM at the fovea is unique, as it is very thin. The foveal ILM is detectable in ILM whole mounts after immunostaining for collagen IV or laminin as a distinct circular area. AFM measurements showed that the foveal ILM has a thickness of approximately 100 nm, whereas the parafoveal ILM has a thickness of up to 3 μm (Figure II.E-5) [15]. The *in vitro* data are consistent with earlier TEM reports [16] (Figure II.E-5b–e), showing a very thin ILM at the fovea and a much thicker ILM at parafoveal regions. The very thin ILM at the fovea and near large blood vessels in the nerve fiber layer [17] suggests that both areas are possible exit points for retinal cells to migrate and then proliferate and form premacular membranes as well as possible entry sites of macromolecules and viruses from the vitreous into the retina.

B. Biochemical Composition of the ILM

The ILM is a basement membrane (BM). BMs are extracellular matrix (ECM) sheets that underlie all epithelia in the body and outline muscle fibers and the vascular endothelium. As such,

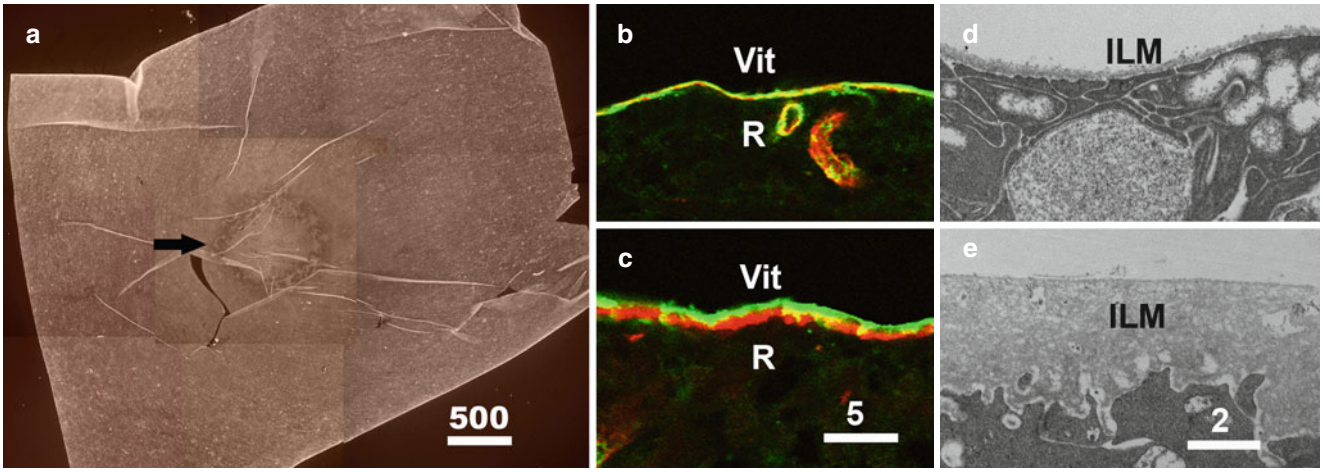

Figure II.E-5 The ILM of the fovea. (**a**) ILM whole mount from the foveal area of a retina, stained for collagen IV. The fovea is detectable (*arrow*) as a distinct circular area in the center of the ILM preparation. (**b**) Fluorescence micrograph showing cross section of the human retina at the foveal center and at the parafoveal area of the same retina. (**c**) The sections were stained for laminin (*red*) and collagen IV 7S α3 (*green*). The foveal ILM is very thin, and the laminin and collagen IV layers seem to blend and overlap. In contrast, the parafoveal ILM (**c**) is thick and the laminin and collagen IV layers are clearly distinguishable. (**d**) TEM micrograph of the human retina in the center of the fovea and at a parafoveal area. (**e**) The foveal ILM is approximately 100 nm thin, whereas the parafoveal ILM has a thickness of over 2,000 nm (Bars: **a**: 500 μm; **b**, **c**: 5 μm; **d**, **e**: 2 μm)

the ILM has similar molecular constituents as other BMs. The identification of BM proteins has been complicated by the fact that BMs are not easily isolated in large quantities. Further, the fact that their protein components are highly insoluble in physiological salt concentrations precludes conventional biochemistry and thus is not a useful approach for BM protein analysis.

It was the discovery of two murine yolk sac tumors that synthesize large quantities of a BM like ECM [18–20] that led to the identification of the dominant BM proteins, including laminin-111 [21, 22], nidogen-/entactin-1 [23, 24], perlecan [25], and collagen IV α1/α2 [26]. In contrast to *in vivo*-derived BMs, the mouse tumor matrix can be solubilized, its components isolated, and its peptide sequenced by conventional biochemistry [27]. More BM proteins were later discovered by means of monoclonal antibodies and by using homology cDNA cloning [28, 29]. Data showed that all of the previously discovered major BM proteins are members of larger protein families. These include the heterotrimeric laminins with five different α-chains, three β-chains, and three γ-chains that form over ten trimeric members [30, 31]. The heterotrimeric collagen IV family members are composed of six genetically different α-chains that assemble into three stable collagen IV trimers [32]. Additional BM components are nidogen-/entactin-1 and nidogen-/entactin-2 [33], and perlecan, agrin, and collagen XVIII are the three dominant BM-associated proteoglycans [34]. All BM proteins are high-molecular-weight proteins of at least 150 kD. The laminin trimers have a molecular weight of 1,000 kD, the collagen IVs over 600 kD, and the proteoglycans between 300 and 600 kD.

Traditionally, protein analysis of BMs in situ was done by immunostaining using antibodies to candidate proteins that are usually present in BMs [35, 36]. More recently, proteomic analysis has been employed for definitive and more comprehensive identification of all BM proteins [13, 37]. Proteomic data from embryonic chick and human ILM, lens capsule, and Descemet's membrane showed that all of these BMs consist of approximately 20 proteins with multiple laminins, multiple collagen type IVs, nidogen-/entactin-1 and nidogen-/entactin-2, and agrin, perlecan, and collagen XVIII. The predominant protein in human ILM is a collagen-type IV, with a chain composition of α3/α4/α5. It is of note that the human lens capsule and BMs of the retina vessels have little collagen IV α3/α4/α5 but an abundant amount of collagen IV α1/α1/α2 [37]. The dominant laminin family member is laminin 521, and the most prominent proteoglycans in the ILM is perlecan, followed by agrin and collagen XVIII [37]. The proteoglycans are responsible for the high water content in the ILM and vitreous [12, 38].

C. Biosynthesis and Assembly of the ILM

All BM proteins are multi-domain molecules that polymerize (laminins, collagen type IVs), cross-link (collagen type IVs), or bind to each other (laminin, agrin, nidogen/entactin, perlecan, collagen type IV). The evidence of polymerization, the mutual binding, and high resolution TEM imaging of individual BM proteins led to a model of BM structure that postulated a two-dimensional network of collagen type IV that combines with a layer of side-to-side polymerized laminin. Nidogen-1 has binding sites for laminin and collagen type IV and was proposed to connect the two polymers [39–43]. Recent data are not entirely consistent with this model,

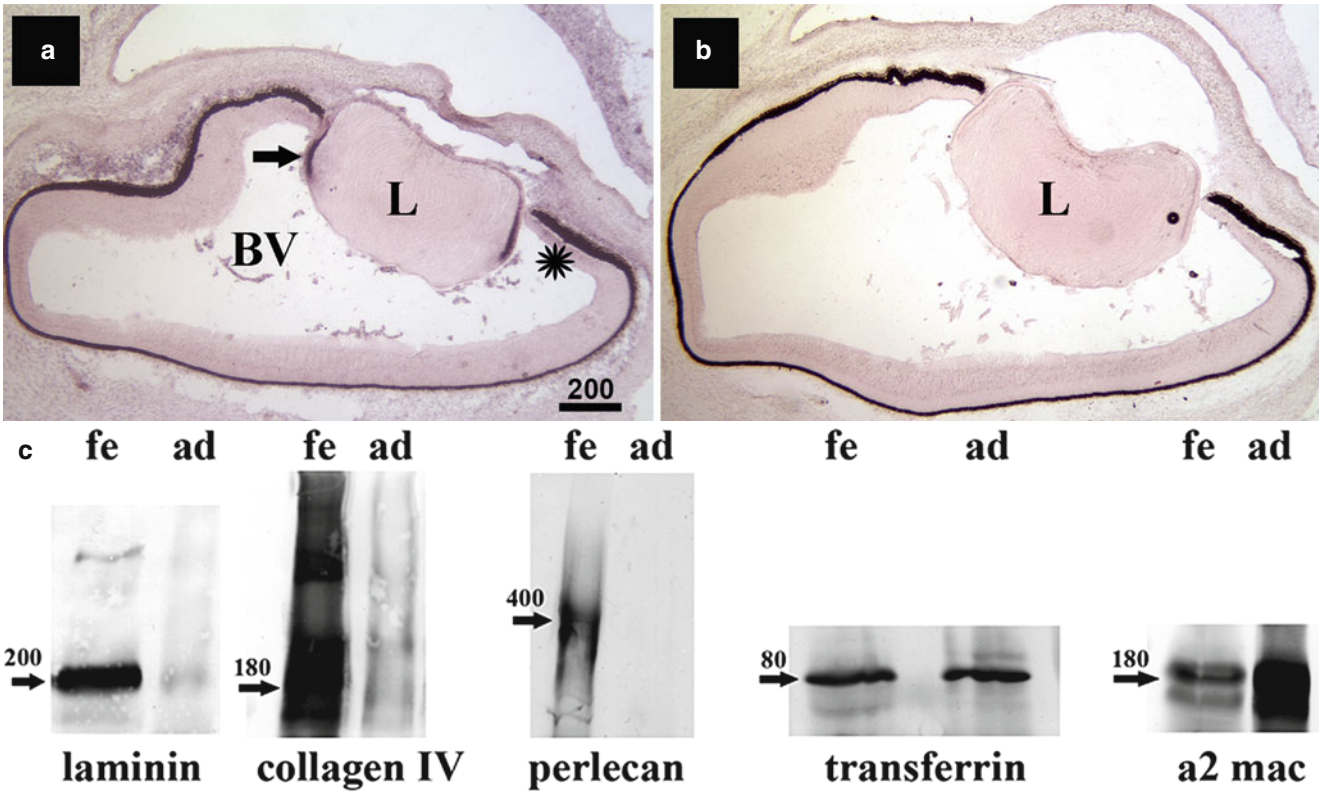

Figure II.E-6 Origin and biosynthesis of the human ILM. *In situ* hybridization. (**a**) Section of a 10-week-old fetal human eye hybridized *in situ* with antisense RNA for the detection of nidogen-1 mRNA. The nidogen-/entactin-1 protein is a major component in the human ILM. The labeled cells expressing nidogen/entactin mRNA are located in the lens epithelium (*arrow*), the ciliary body (*star*), and the endothelium of the hyaloid vasculature (*BV*). The absence of any detectable label in the retina indicates that the synthesis of this ILM protein occurs in extraretinal tissues, such as the lens, ciliary body, and intravitreal vasculature. (**b**) Control section of the same fetal eye labeled with nidogen-/entactin-1 sense RNA. The *in situ* data suggest that ILM proteins should be detectable in the fetal vitreous. (**c**) Western blots of fetal (*fe*) and adult (*ad*) vitreous showed that BM proteins are indeed abundant in fetal stages of human eye development and very low in the adult. The blots also showed that transferrin, a non-ILM protein, is not downregulated in the adult eye and that α2 macroglobulin, a typical serum protein, is even more abundant in the adult than in the fetal human vitreous. The data combined indicate that BM protein synthesis occurs in nonretinal tissues of the eye. It is high in fetal stages and selectively downregulated to very low levels in the adult human eye (Bar: **a**, **b**: 200 μm). *L* lens

particularly the finding that BMs assemble properly in the absence of nidogen-1 [44, 45].

Because of the propensity for proteins to polymerize, it was previously thought that BMs spontaneously assemble when BM proteins are present at sufficiently high concentrations [46]. It later became clear that cell receptors are also required for BM assembly. Cell receptors for BM assembly are members of the integrin family and dystroglycan. The best evidence for a central role of cellular receptors in BM assembly comes from targeted mutations of dystroglycan and integrins in mice that lead to defects in BM assembly, which are very similar to BM disruption caused by mutations of essential BM proteins [47, 48].

The presence of the ILM adjacent to the end feet of the Müller glial cells suggested that the retina, specifically Müller cells, is the major source of ILM proteins. However, with the exception of the mRNA for agrin, ILM protein mRNAs were not detected in the neural retina [49–52]. Since the ILM is composed of secretory proteins, however, the origin of ILM proteins could theoretically be any cell layer lining the interior of the eye. Indeed, in situ hybridization of embryonic mouse and human eyes revealed that almost all ILM proteins are synthesized by the lens epithelium, the future ciliary epithelium, and the endothelial cells of the hyaloid vasculature (Figure II.E-6) [49, 50, 53, 54].

The in situ hybridization data suggested the hypothesis that ILM proteins are secreted by the lens and ciliary body into the vitreous and that they diffuse to the retinal surface where they assemble into the ILM. The hypothesis further proposes that the role of the retina is to provide the cell surface receptors of the neuroepithelial cells for ILM assembly. In support of this hypothesis, studies have shown that large quantities of laminin, collagen IV, nidogen, perlecan, and agrin are present in the embryonic chick and fetal and neonatal human vitreous. The highest concentrations of ILM proteins in the vitreous coincide with the timing of most active ILM assembly during rapid eye growth [53, 54]. The analysis of the vitreous also showed that the concentrations of ILM proteins decline to very

low levels in the adult human vitreous, and an extended study in chick showed a precipitous decrease of the ILM protein synthesis at late fetal/neonatal stages [53, 55]. The current data suggest that the ILM is primarily assembled during embryonic, fetal, and neonatal stages of development and that this activity is greatly reduced in the adult life. However, given the continuous increase in human ILM thickness during aging, it is probable that there is continued low level of the ILM protein synthesis throughout life.

It is currently not known if the ILM regenerates. The fact that the expression of human vitreous proteins undergoes similar age-related downregulation as ILM proteins and that the vitreous gel does not regenerate after vitrectomy suggests that a complete ILM regeneration does not occur. Consistent with this proposition is experimental data in rabbits showing that a damaged ILM does not regenerate [56]. On the other hand, it has recently been shown that *in vitro* Müller cells can synthesize ILM collagens [57]. Furthermore, studies in monkey found that ILM peeling is followed by resynthesis of the ILM over the course of several months [58].

D. Role of the ILM in Ocular Development

It is of great interest to note that during ocular embryogenesis the ILM can be readily identified during invagination of the optic vesicle (Figure II.E-7). Just prior to completion of invagination, it can be clearly appreciated that there is continuity of the ILM and Bruch's membrane. This suggests that although these two BM interfaces are considered separate and distinct entities, their origin is likely coded by the same genes and their composition is likely identical, at least at the origin of life. Thus, phenomena such as aging, glycosylation, cell adhesion, cell migration, and cell proliferation at these two sites share a common pathway, at least as it concerns the underlying BM substrate upon which these processes occur [59, 60].

The ILM is essential in early ocular and retinal development. Evidence comes from the retinal phenotype of a series of targeted deletions of BM proteins, their processing enzymes, and their receptors in mice and a number of spontaneous mutations in humans. Targeted mutations of the genes encoding laminin chains [61–63] or the binding site of laminin γ-1 for nidogen-/entactin-1 [53], collagen IV [64], and enzymes responsible for the glycosylation of dystroglycan, such as LARGE, fukutin, fukutin-related protein, POMT1 and POMT2, and POMGnT1 [65–67], cause major breaks in the ILM and result in retinal ectopia. In eyes with these mutations, retinal cells migrate through breaks in the ILM into the vitreous (Figure II.E-8a–d). Further, approximately 50 % of the retinal ganglion cells undergo apoptosis, resulting in major optic nerve hypoplasia [53]. The underlying cause for this retinal dysplasia is that the mutations cause a weakening of the biomechanical strength of the ILM, leading to breaks in the ILM due to the rapid expansion of the retina during development. The breaks in the ILM are accompanied by the retraction of the neuroepithelial cells, most likely the cause of ganglion cell death and optic nerve hypoplasia [53]. AFM measurement showed that the stiffness of the ILM in these mutations is lowered by at least 50 %, explaining the numerous stretch-related breaks in the ILM (Figure II.E-8e, f). Similar retinal phenotypes are also recorded for spontaneous mutations of Walker-Warburg syndrome, muscle-eye-brain diseases, and Fukujama muscular dystrophy in humans [68–71].

In addition to massive eye phenotypes, the mutations also affect brain development and, in many cases, result in muscular dystrophy and rupture of ocular and cerebral blood vessels [65, 72–74]. The retinal, cortical, vascular, and muscular phenotypes provide strong evidence that the mechanical strength of BMs is essential in the development of the retina, cerebral cortex, blood vessels, and muscles.

The ILM can be peeled off in the adult human eye and represents a medical intervention for macular hole closure and the cure of other vitreomaculopathies. Peeling the ILM assures removal of an abnormal posterior vitreous cortex and other pathologic membranes. This is only innocuous when partial thickness of the ILM is removed. Further, the ILM is probably regenerated, at least in part, by Müller cells during the months following surgery.

E. Aging of the ILM

Like many connective tissues of the human body, the ILM changes its molecular composition and structure with age. Biochemically, age-related variations were observed in the relative concentration of laminin, which is higher during early stages of ILM assembly than later, and the relative concentration of collagen IV that increases with age [13, 37]. This may underlie the most obvious age-related change of the human ILM, that being an age-dependent increase in thickness with progressing age. During fetal stages, the ILM has a thickness of less than 100 nm and the classical trilamellar BM structure of BMs (Figure II.E-2c). This changes with aging, as the ILM becomes thicker and loses its trilaminar structure to become amorphous (Figure II.E-9). Further, the retinal side of the ILM develops indentation that become more dramatic with progressing age. A systematic analysis of ILMs from over 20 patients (Figure II.E-9f) shows the progressive increase in the ILM thickness with advancing age [4]. The continued age-related increase in the ILM thickness indicates that ILM protein synthesis occurs in the adult human eye over the entire life span but at a very reduced level. The absolute number of years of age counts to a major degree, since increases in the ILM thickness have only been recorded for the long-lived humans and primates and not in any of the short-lived animal species [75].

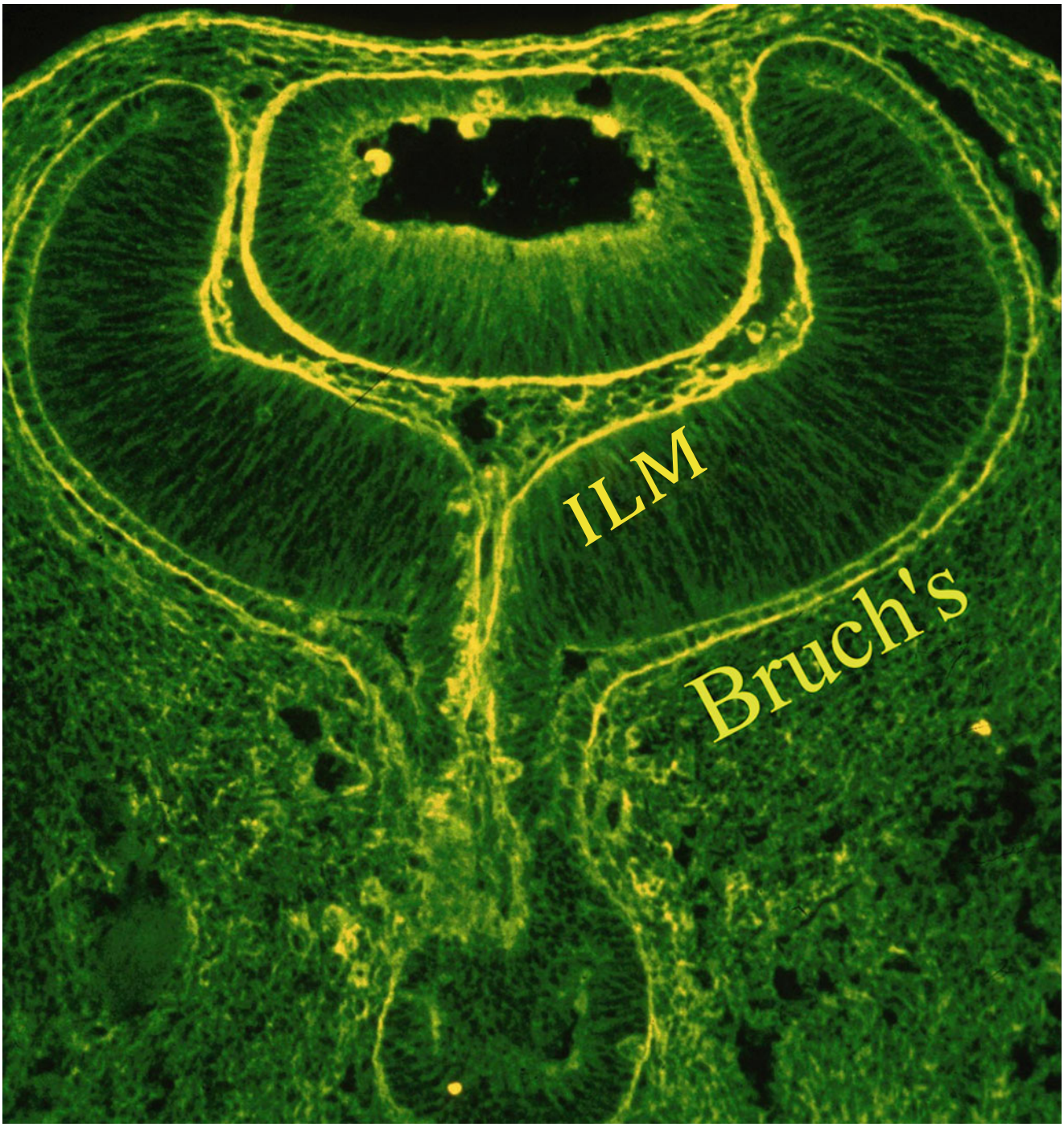

Figure II.E-7 Immunohistochemistry of the human embryonic eye following invagination of the eye cup at about 8 weeks gestation. The section is stained with immunofluorescent antibodies to *Agaricus bisporus* (ABA) that intensely stain basement membranes. The *yellow line* labeled "Bruch's" is the chorioretinal interface destined to become Bruch's membrane, while the *yellow line* labeled "ILM" (*inner limiting membrane*) is the vitreoretinal interface destined to become the ILM. Note that the two structures are continuous and represent the same identical membrane folded over inside the eye. Thus, pathologic events such as cell migration and proliferation at these two interfaces are occurring upon the same identical substrate (Courtesy of Dr. Greg Hageman)

In addition to an increase in thickness, the ILM also becomes stiffer with advancing age [4]. It is conceivable that the progressive change in the protein composition to more collagen IV and less laminin is responsible for this age-related increase in the ILM stiffness.

F. Role of the ILM in Disease

1. ILM and Diabetes

Diabetes alters tissues throughout the body via nonenzymatic glycosylation of proteins. This has been demonstrated

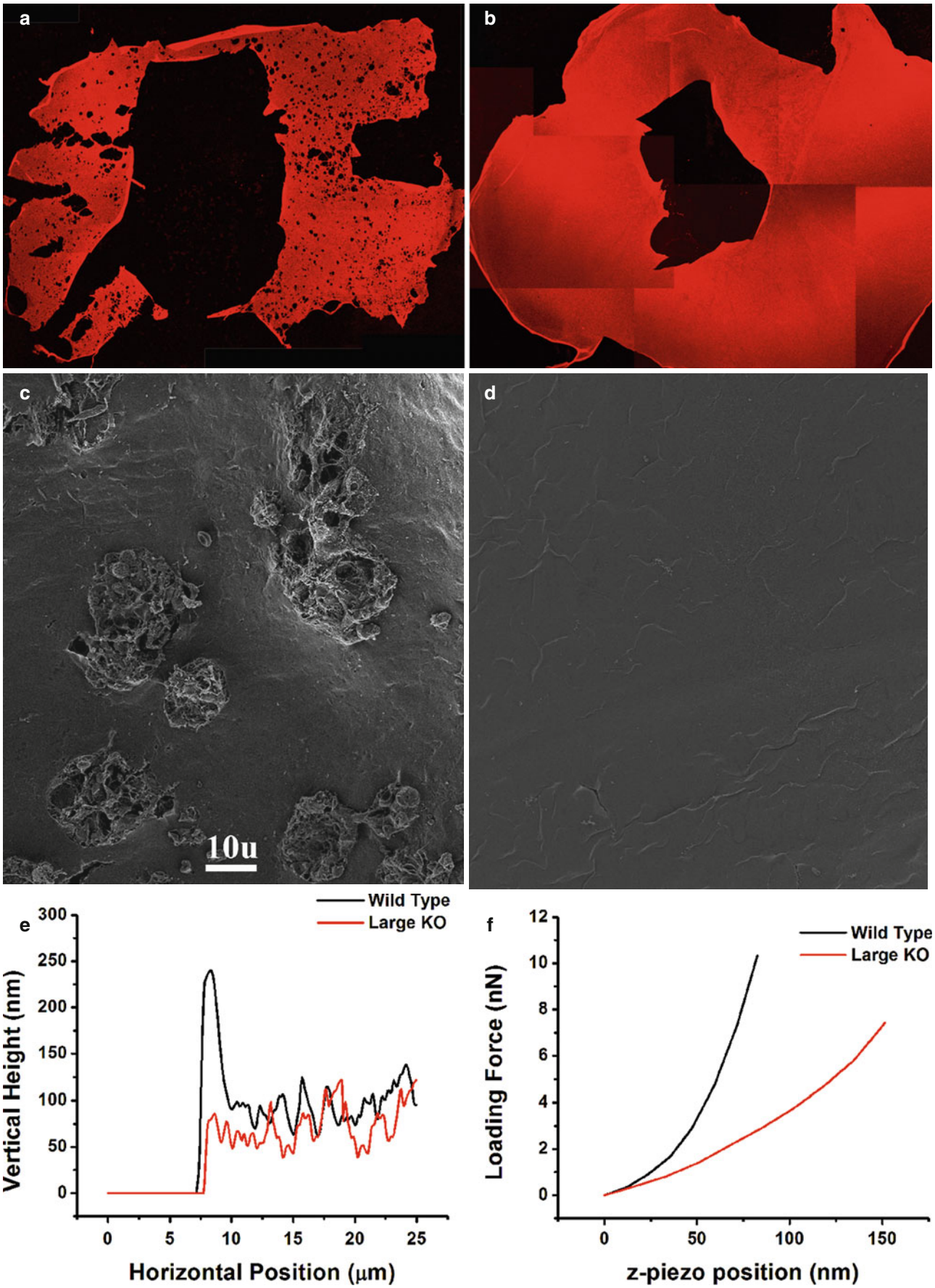
a
b
c
10u
d
e
Wild Type
Large KO
Vertical Height (nm)
300
250
200
150
100
50
0
0
5
10
15
20
25
Horizontal Position (μm)
f
Wild Type
Large KO
Loading Force (nN)
12
10
8
6
4
2
0
0
50
100
150
z-piezo position (nm)

Figure II.E-8 Biomechanical properties of the ILM and retinal development. Mice with a targeted mutation of LARGE or POMGnT1 have fragile BMs. Both mutations affect enzymes that are essential for the glycosylation of dystroglycan, one of the receptors for laminin that is essential for BM assembly. (**a**) An ILM flat mount from a neonatal mouse with a homozygous mutation for either of the two enzymes shows numerous holes as the ILM is fragile and ruptures during eye growth. (**b**) An intact control ILM from a heterozygous mouse. (**c**) SEM images of the vitread surface of retinas from a mutant animal show the multiple ruptures in the ILM that lead to the migration of retinal cells into the vitreous. (**d**) The continuous and smooth surface of the ILM from control retina. (**e**) AFM height measurements showed that the ILM from the mutant mouse is slightly thinner. (**f**) Stiffness measurements showed a dramatically weaker ILM from the mutant mouse as compared to the control mouse ILM (Bar: **c**, **d**: 10 µm)

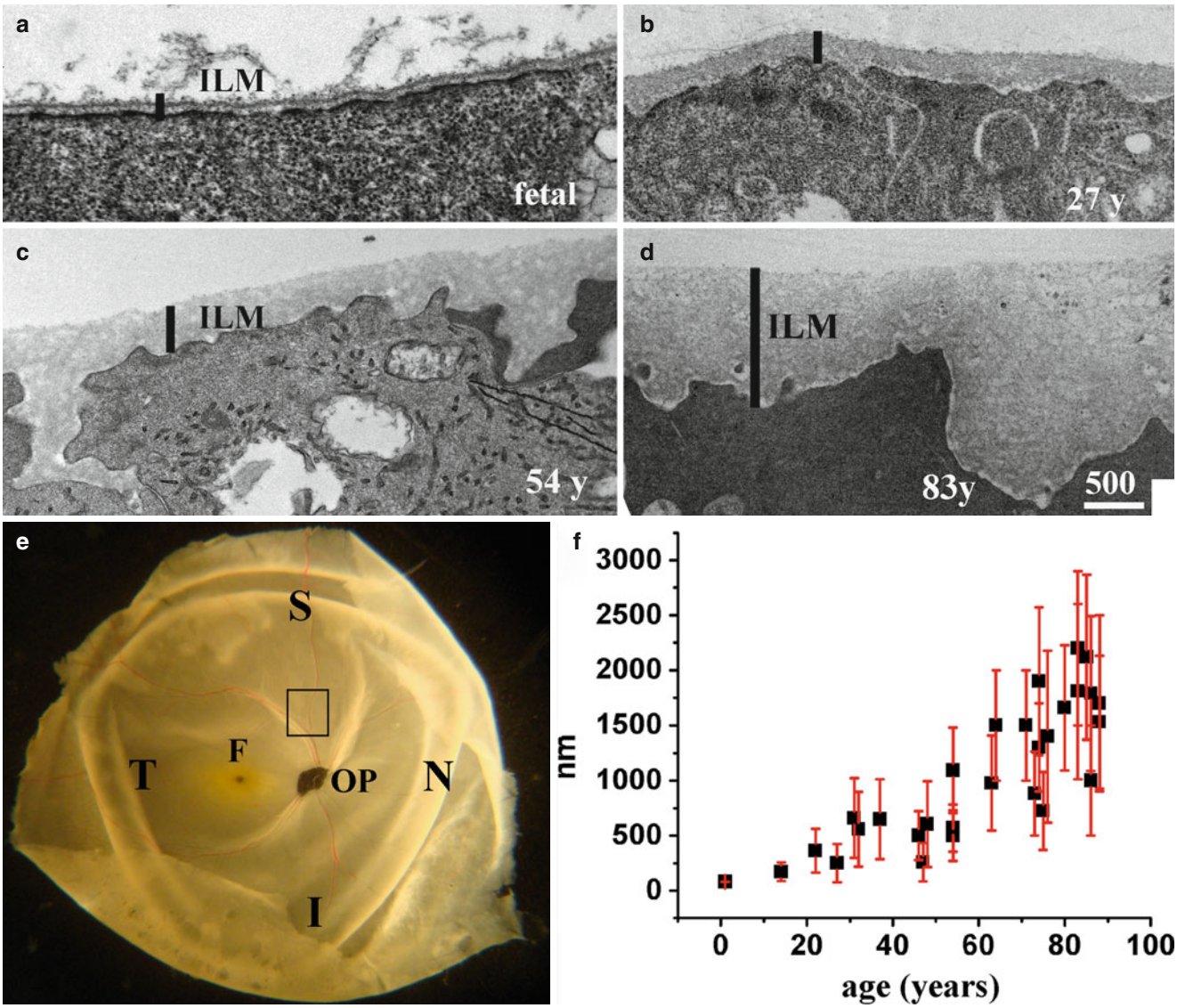

Figure II.E-9 Age-dependent increase in ILM thickness. TEM micrographs show the vitread surface of the retina from a 16-week fetal human eye (**a**) and from 27, 54 and 83-year-old adult human eyes (**b**–**d**). The ILM from the fetal eye (**a**) has the typical morphology of a BM – it is 70 nm thick with a typical lamina densa and three-layered ultrastructure. Between 22 and 83 years of age (**b**–**d**), the ILM dramatically increases in thickness, becomes highly irregular at its retinal surface, and no longer contains a distinct lamina densa. The black bars in (**a**) to (**d**) indicate the thickness of the ILM. Panel (**e**) shows an adult human retina with the location in the superior posterior pole of the right eye (*boxed*) where the retina was sampled. The graph in panel (**f**) shows the age-dependent increase in ILM thickness. Each of the data points represents averages from measurements of one pair of eyes of a single patient. *F* fovea, *OP* optic papilla, *S* superior, *I* inferior, *T* temporal, *N* nasal (Bar: **a**–**d**: 500 nm)

to alter vitreous molecules [76, 77] and structure [78], and the term "diabetic vitreopathy" has been proposed to refer to these effects [79] (see chapter I.E. Diabetic vitreopathy). Insofar as the ILM is similarly proteinaceous, advanced glycosylation end products could accumulate in this tissue and alter its physiology.

It is well established that BMs increase in thickness during long-term diabetes. This applies also to the ILM [80–82]. The increase in the ILM thickness occurs in patients suffering from type 1 and type 2 diabetes (Figure II.E-10). However, the increase in thickness is only detectable after several years of the diabetes condition and is not detectable in diabetic mice [83]. What is presently still unknown is the nature of the proteins that are responsible for diabetes-related BM thickening. It is possible that the normal BM proteins are excessively synthesized and incorporated into the ILM at an accelerated rate or that new, diabetes-specific proteins are expressed and incorporated leading to an altered, diabetes-specific protein composition of the ILM. There are some findings that support the latter: fibronectin, normally not present in the human ILM, is detected in ILMs from diabetic eyes [35, 82]. However, several studies have also shown that collagen IV is excessively synthesized in long-term diabetes, which would indicate that normal ILM proteins are expressed at a higher than normal rate [84]. It is of note that only negligible differences in protein compositions of the ILM were detected in diabetic mice showing that mouse models are inadequate to study the diabetic-related pathological changes that are detectable in long-term diabetic human patients [83].

2. Proliferative Diseases and the ILM

Cell proliferation at the vitreoretinal interface plays an important role in proliferative diabetic retinopathy, proliferative vitreoretinopathy (see chapter III.J. Cell proliferation at vitreo-retinal interface in PVR and related disorders), and macular pucker formation (see chapter III.F. Vitreous in the pathobiology of macular pucker). The interaction of the involved cell, which differs in each condition, with the underlying substrate can influence the course of the disease. This is critical to our understanding of disease pathogenesis with respect to cell adhesion, cell migration, and cell proliferation.

Under normal conditions the vitread surface of the human retina is cell-free (Figure II.E-11a, b). However, there are various age- and disease-related conditions where membranes form on the retinal surface. Foos [16, 17] termed these epiretinal membranes, although this is a misnomer since the term "epiretinal" is not adequately specific. Subretinal membranes are also "epiretinal." The membranes in question here are all actually "premacular" (Figure II.E-11c–e). Foos further described that these membranes arise via cell migration from the retina through the ILM. While this is probably true in proliferative diabetic retinopathy, where there is migration and proliferation of vascular endothelial cells arising from the retina, and proliferative vitreoretinopathy, where retinal pigment epithelial cells play an important role (although they don't traverse the ILM but rather enter vitreous via breaks in the retina) [17].

This is not true for macular pucker, the most common case of premacular membrane formation that disturbs vision. Premacular membranes that cause macular pucker most often result from anomalous posterior vitreous detachment [85, 86] with vitreoschisis [87–90] (see chapter III.B. Anomalous PVD and vitreoschisis). The hyalocytes that are embedded in the outer posterior vitreous cortex are left attached to the retina and elicit monocyte migration from retinal vessels as well as glial cell migration from the retina to form the premacular membranes that contract and induce macular pucker. The contractile forces that induce this pucker likely originate from hyalocytes (see chapter II.D. Hyalocytes).

The ILM plays an important role in proliferative disorders at the vitreoretinal interface in several ways. The formation of cellular membranes on the retinal surface requires the migration of cells, their adhesion to a substrate, and then proliferation. Vascular endothelial cell migration through the ILM is important in proliferative diabetic retinopathy as well as trans-ILM migration of glial cells from the retina. Monocytes from the circulation are important in macular pucker. It is not clear whether or not there is alteration of the normal ILM that allows cells to migrate from the retinal vessels, although the foregoing section on diabetes and the ILM would suggest that the ILM in diabetic patients is not normal. In the case of macular pucker, there is no evidence that the ILM is abnormal.

Cell adhesion to normal or pathologic surfaces is mediated by laminin [91]. In the eye, laminin has been shown to play a critical role in retinal vascular development [92], and it would seem a reasonable extrapolation to implicate similar roles in pathologic neovascularization. Thus, the attributes of the ILM and its impact on cell adhesion are important considerations. Studies [93] have shown that the human ILM has side-specific properties that are detectable by side-specific labeling of a flat-mounted ILM preparation using antibodies to laminin or collagen IV. Laminin is most abundant on the retinal side of the ILM, whereas an antibody to the 7S domain of collagen IV α3 labels the vitread side (Figure II.E-12a–c). When dissociated MDCK, corneal, or retinal cells were plated on flat-mounted and folded ILMs, the cells adhered preferentially to the retinal side of the ILM (Figure II.E-12d). This finding suggests that there is a change in proliferative pathologies that facilitates cell adhesion to the vitread side of the ILM. Alternatively, the presence of remnant posterior vitreous cortex on the ILM as a result of anomalous PVD with vitreoschisis could provide the substrate needed for cell adhesion and subsequent proliferation. Contractile effects upon the retina would then arise from this layer of remnant posterior vitreous cortex that has become hypercellular and is still attached to the ILM via the intervening ECM, called the vitreoretinal border region by Heergaard (see above).

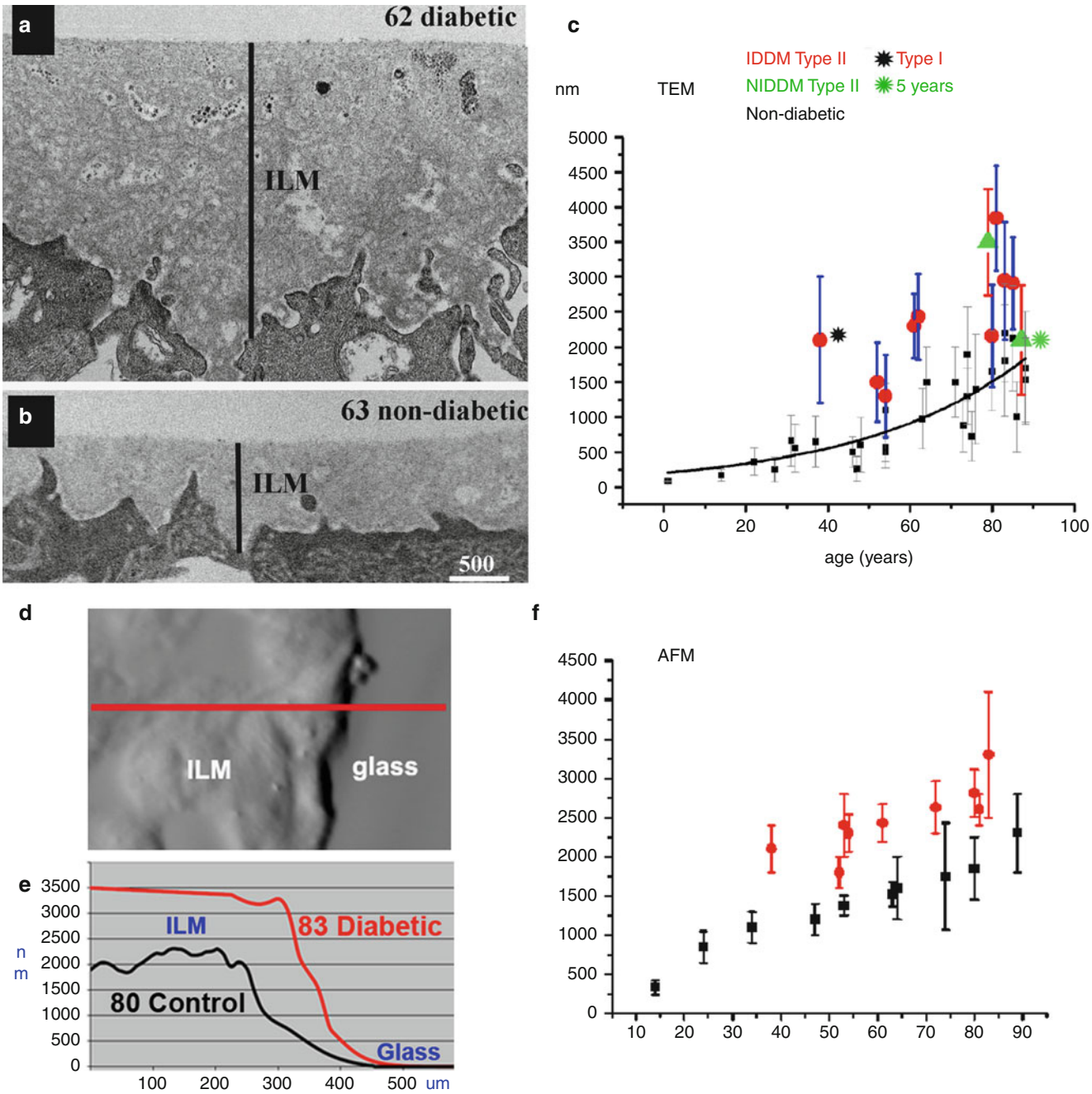

Figure II.E-10 Diabetes-related increase in ILM thickness. (**a**) TEM micrograph of ILM from a 62-year-old diabetic patient. (**b**) TEM micrograph of ILM from a 63-year-old nondiabetic patient. (**c**) Graph showing that the thickness of ILMs increases with age, but the thickness of ILMs from diabetic patients is approximately double the thickness of ILMs from age-matched nondiabetic subjects. (**d**) A similar difference in the thickness of diabetic and nondiabetic ILMs was detected by probing the ILM samples with atomic force microscopy (*AFM*). An AFM image of the edge of an ILM from a diabetic patient is shown. The ILM had been flat mounted on a glass slide, and the glass surface served as a reference for the height measurements. The *red line* indicates the trace of the AFM probe used to determine the thickness of the sample. (**e**) Representative height traces of a diabetic and a nondiabetic ILM quantitatively demonstrate the increased thickness of the ILM in diabetic patients. (**f**) AFM thickness measurements of nondiabetic and diabetic ILMs show that diabetic ILMs (*red*) are on average twice as thick as ILMs from similarly aged nondiabetic subjects (Bar: **a**, **b**: 500 nm). Notes: The patient's medical history, time of harvesting of eyes after death, and the time of tissue delivery to the laboratory are available for every ILM sample analyzed in this graph. Except for the sample marked by a star, all samples came from patients with type II diabetes. The duration of diabetes was at least 10 years, except for the ILM marked by a green star (5 years). *IDDM* insulin-dependent diabetic, *NIDDM* non-insulin-dependent diabetic

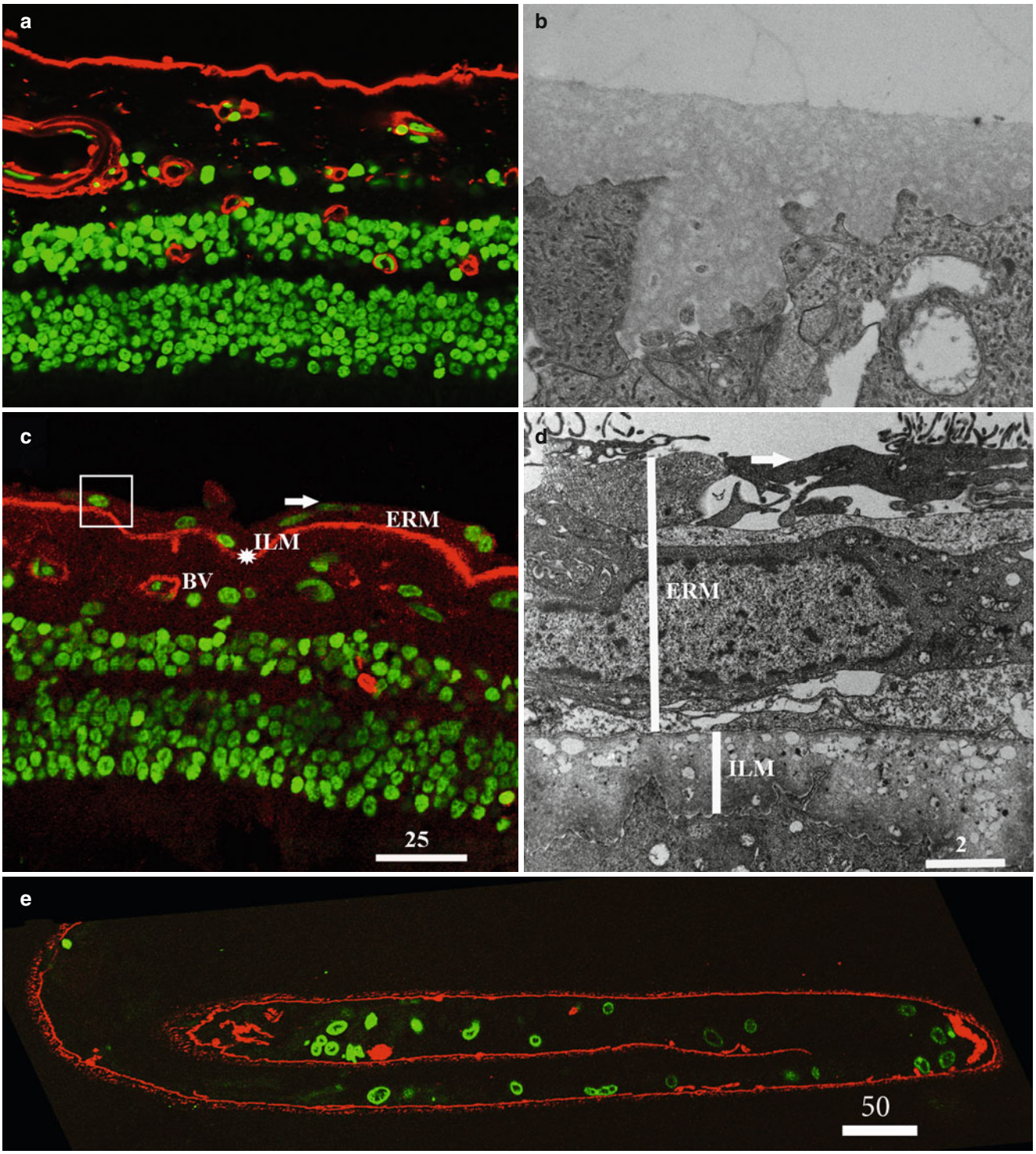

Figure II.E-11 Premacular ("epiretinal") membranes. The vitread surface of the ILM from a normal human retina is cell-free as shown by immunostaining for collagen IV (**a**; *red*) or by TEM (**b**). (**c**) A premacular cell layer is detectable in a cross section by staining the specimen for collagen IV (*red*) and cell nuclei (*green*) or by TEM (**d**). (**e**) A surgical specimen following ILM peeling shows the excised ILM with attached cells stained for collagen IV (*red*) and cell nuclei (*green*) (Bars: **a**, **c**: 25 μm; **b**, **d**: 2 μm; **e**: 50 μm)

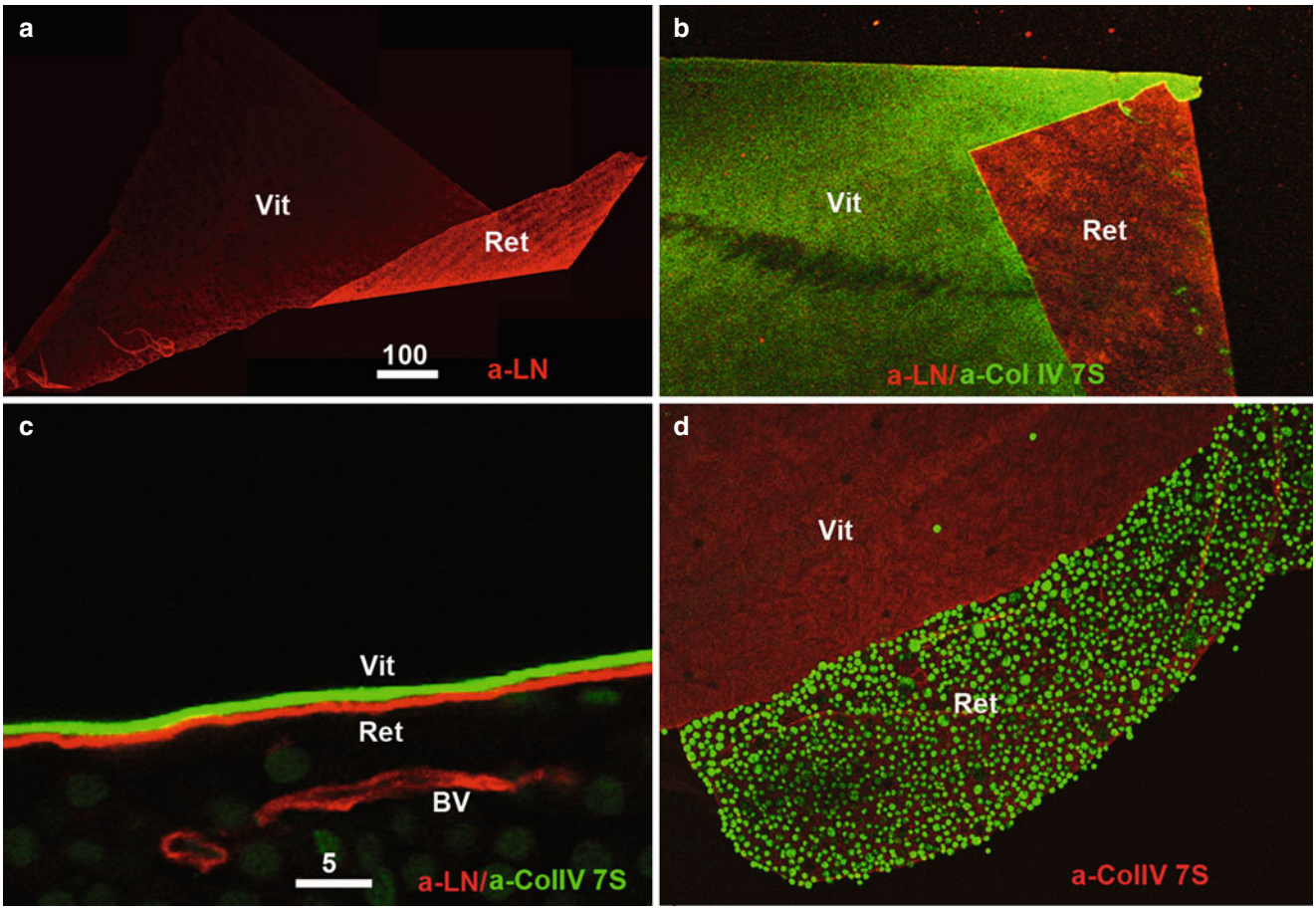

Figure II.E-12 Cell adhesion on the ILM. The human ILM has side-specific properties that are detectable by the side-specific labeling of a flat-mounted ILM using antibodies to laminin (**a**, **b**) or collagen IV (**b**, **c**). Laminin is most abundant on the retinal side of the ILM (**a**, **b**), whereas an antibody to the 7S domain of collagen IV a3 labels the vitread side (**b**, **c**, *green*). The abundance of both proteins on either the retinal or vitread side is best appreciated by double labeling (**b**, **c**). When dissociated MDCK, corneal, or retinal cells were plated on flat-mounted and folded ILMs, the cells adhere preferentially to the retinal side of the ILM (**d**). The vitread side of this preparation was labeled with an antibody to the 7S domain of collagen IV a3 (*red*). The adherent cells were labeled *green*

3. Tractional Disorders and the ILM

The ILM is the site of pathologic traction at the vitreoretinal interface. Traditionally, this has been conceived as axial in direction, resulting in anteroposterior traction upon the retina. Gass [94] first proposed that tangential traction at the vitreoretinal interface can also disturb the macula and reduce vision via distortions (macular pucker), blurring (macular edema), and/or scotomata (macular hole). It is not clear whether these tangential forces are exerted uniquely by the posterior vitreous cortex or whether the ILM plays a role as well. Thus, the biophysical properties of the ILM are important to study so as to elucidate this potential role.

a. Biophysical Properties of the ILM

Biophysical properties, such as elasticity and stiffness, are important determinants of the ILM role in disease. For elasticity studies and stiffness measurements, the ILM has to be isolated as a clean preparation, which is done by dissolving the retinal tissue in detergent [4, 93, 95–97]. These ILM sheets are transparent and invisible under bright-field illumination but detectable under dark-field illumination (Figure II.E-13a, lower left-hand corner inset). Isolated ILMs have the ultrastructure of ILMs in situ, with a smooth vitread surface and an indented and irregular retinal surface (Figures II.E-13a, b). Interestingly, the ILM sheets scroll, with the retinal side consistently facing outward and the vitread surface inward (Figure II.E-13a). This scrolling phenomenon with the epithelial side on the outside of the scroll and the connective tissue side on the inside of the scroll is also observed for the lens capsule and Descemet's membrane of the cornea, thus suggesting an inherent property of BMs [97]. AFM showed that the retinal side of the ILM is at least twice as stiff as the vitread side [15, 93].

It is important to appreciate that during any vitreous surgery that includes ILM peeling, this scrolling effect is only observed when full-thickness ILM is surgically removed

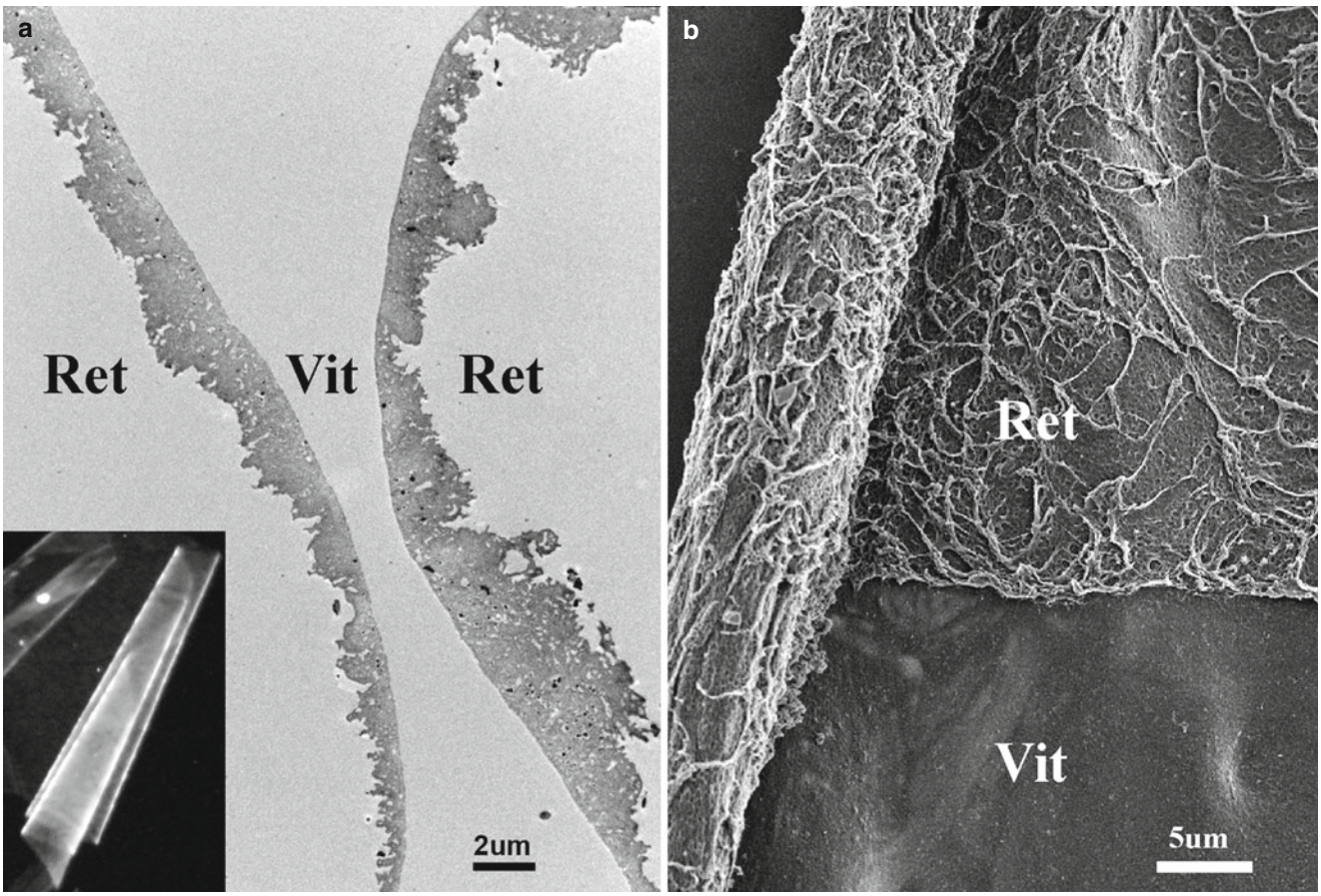

Figure II.E-13 Isolated human ILM. ILMs can be isolated from human retina by dissolving the retinal cells in detergent. The detergent-insoluble BMs are collected under a dissecting microscope using dark-filed illumination (**a**, *insert*). The isolated ILMs scroll up with the retinal surface facing outward and the vitread surface facing inward. TEM (**a**) and SEM (**b**) micrographs of isolated ILMs show that the retinal surface (*Ret*) is highly irregular, whereas the vitread surface (*Vit*) is even and smooth. The images also show that the ILM preparations are clean and not contaminated with cellular debris or non-BM ECM (Bar: **a**: 2 μm; **b**: 5 μm)

from the retina. This is fortunately not common, since the overwhelming majority of the time the peeled tissue is partial (not full) thickness ILM, which does not scroll. Thus, splitting of the ILM occurs (perhaps between the lamina lucida interna and the lamina densa) and only the inner (anterior) portion of the ILM is being peeled. This explains why ILM peeling is associated with better surgical outcomes and good vision. Full-thickness ILM peeling will likely not have good postoperative vision due to damage to the underlying retinal nerve fiber layer as well as Müller cells. Thus, surgeons witnessing scrolling of the tissue being peeled off the retina may be well advised to establish a different surgical plane.

The availability of isolated and clean ILM allowed collecting data on its biomechanical properties. By using the force-indentation mode of the AFM, the stiffness of isolated and flat-mounted mouse, chick, and human ILMs were recorded in the high kPA to low MPa range [3, 4]. This corresponds to the stiffness of hyaline cartilage [9] and characterizes the ILM and all other BMs as tough connective tissue structures. It is of note that the stiffness of cell layers is in the low kPa range [98], and thus BM, including the ILM, is several hundred-times more stable than cell layers and explains why cell layers fail when their BMs or BM assembly receptors are defective [67].

4. Uveitis

Abnormalities of the vitreoretinal interface are common in patients with uveitis and include posterior vitreous detachment, preretinal membrane formation, retinal neovascularization, and vitreomacular traction with or without cystoid macular edema [99, 100]. Partial and full-thickness macular holes, although uncommon in patients with uveitis, have also been described and are typically attributed to accelerated anteroposterior or tangential traction forces [101]. More than half of the nearly 60 uveitic macular holes that have been described in the literature have occurred in patients with Behcet's syndrome – although it remains unclear whether the development of macular holes in patients with uveitis in the setting of Behcet's represents a relative predisposition for

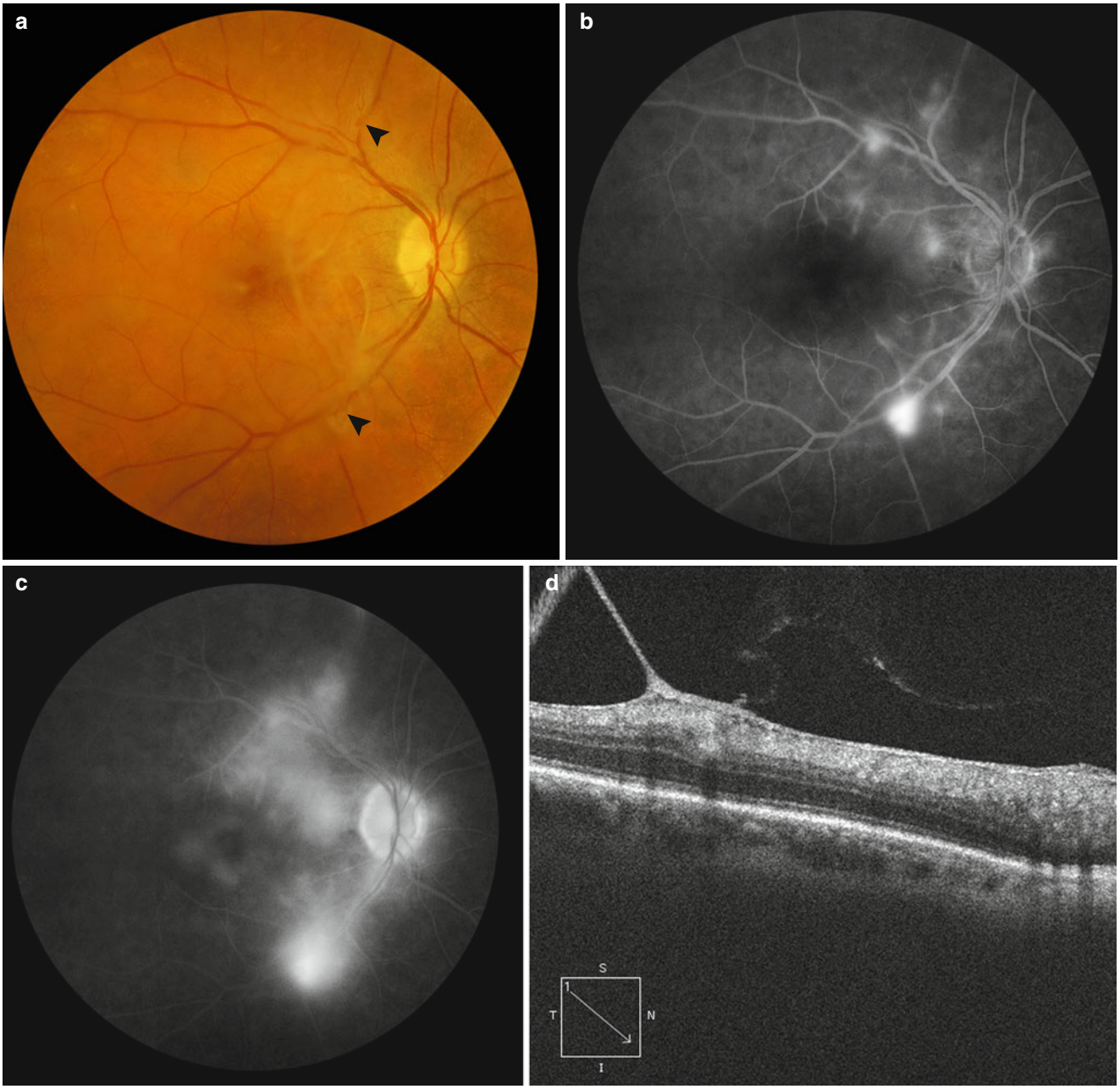

Figure II.E-14 Color fundus photograph (**a**), early (**b**), and late (**c**) fluorescein angiography photographs, and spectral domain ocular coherence tomography (SD-OCT, **d**) of a 63-year-old woman with extensive vitreoretinal traction throughout the posterior pole producing both retinal neovascularization (*arrowheads*) and diffuse retinal vascular leakage mimicking vasculitis. The SD-OCT image was taken along the superior temporal arcade vessels. No vitreous cells were present and a workup for causes of uveitis or vasculitis was unrevealing. The patient had no history of radiation or evidence of diabetes mellitus. Similar findings were present in the fellow eye

macular hole formation [102], related perhaps to intrinsic ILM abnormalities. Sullu and associates recently described a case of widespread vitreoretinal traction involving the macula, optic disc, and major retinal vessels that produced diffuse leakage on fluorescein angiography mimicking uveitic retinal vasculitis [103] (Figure II.E-14). This may relate to the special structural interface between the posterior vitreous cortex and the ILM over retinal blood vessels (see below).

III. Posterior Vitreous Cortex

A. Structure

The posterior vitreous cortex is 100–110 μm thick [104, 105] and consists of densely packed collagen fibrils [104–106] (Figure II.E-15). The term "posterior hyaloid" is often used to refer to this structure, but "hyaloid" is best reserved for the

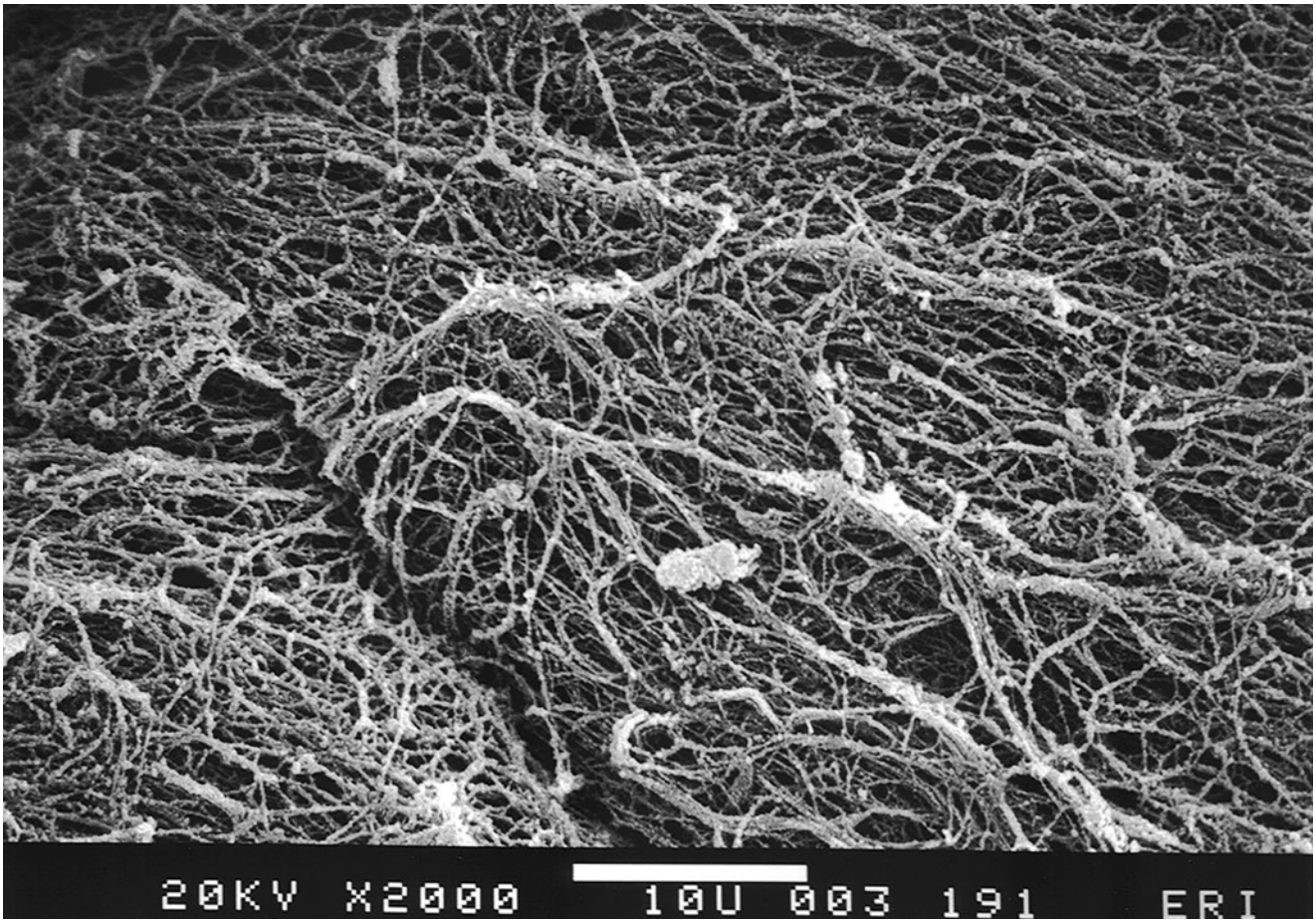

Figure II.E-15 Scanning electron microscopy of the posterior aspect of the human posterior vitreous cortex. Scanning electron microscopy demonstrates the dense packing of collagen fibrils in the vitreous cortex. To some extent this arrangement is exaggerated by the dehydration that occurs during specimen preparation for scanning electron microscopy (Bar = 10 μm) [107]

hyaloid artery present during embryogenesis and "face" is to be reserved for the front of the vitreous, not the back, since the face is on the front of the head not the back. Thus, there is an anterior hyaloid face, but not a posterior hyaloid face.

A lamellar organization of these collagen fibrils results in the appearance of sheets on immunohistochemistry (Figure II.E-16). These potential cleavage planes are important not only as sites of tissue separation during posterior vitreous detachment (see chapter III.B. Anomalous PVD and vitreoschisis), but also as potential cleavage planes during membrane peel surgery. Because of vitreoschisis many experienced surgeons have peeled what was thought to represent full-thickness posterior vitreous cortex membranes, only to find additional membranes still attached to the macula.

There is no posterior vitreous cortex over the optic disc, and the cortex is thin over the macula due to rarefaction of the collagen fibrils, allowing vitreous to extrude and give the appearance of two holes. The premacular hole in the posterior vitreous is sometimes referred to as the premacular bursa. The prepapillary hole in the vitreous cortex can sometimes be visualized clinically when the posterior vitreous is detached from the retina. If the peripapillary glial tissue is torn away during PVD and remains attached to the vitreous cortex about the prepapillary hole, it is referred to as Vogt's or Weiss' ring. Vitreous can extrude through the prepapillary hole in the vitreous cortex (Figure. II.E-17) but does so to a much lesser extent than through the premacular vitreous cortex.

B. Cells of the Posterior Vitreous Cortex

1. Hyalocytes

Reeser and Aaberg [109] considered the vitreous cortex to be the "metabolic center" of vitreous because of the presence of hyalocytes. These cells were first described in 1845 by Hannover. Schwalbe [110] placed these cells into the group of "Wanderzellen" (wandering cells, *i.e.*, leukocytes or macrophages) on the basis of their morphology, distribution, and behavior. He later named them "subhyaloidale Zellen" [111]. Balazs [112] modified this term and named the cells "hyalocytes." The origin of hyalocytes is unknown, although

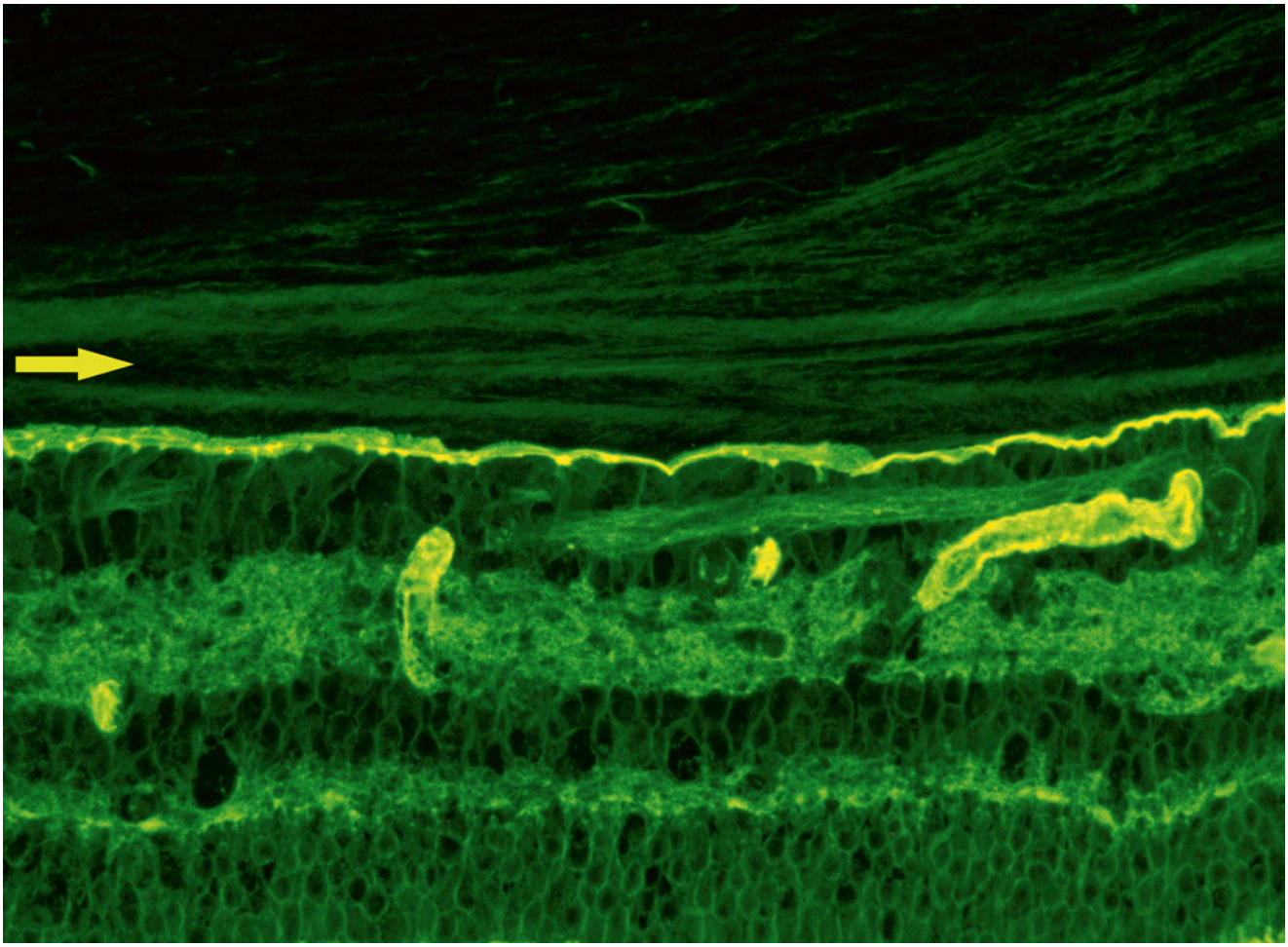

Figure II.E-16 Lamellar organization of the posterior vitreous cortex in the monkey. Immunohistochemistry with anti-ABA lectin antibodies of the monkey vitreoretinal interface demonstrates lamellae in the posterior vitreous cortex (*arrow*) just above the ILM of the retina (intensely staining *yellow line*). These lamellae represent potential cleavage planes during anomalous PVD with vitreoschisis (Courtesy of Greg Hageman, PhD; Reprinted with Permission [90])

Balazs considered them to be remnants of the adventitia of the hyaloid blood vessels that fill the vitreous body early during embryogenesis. Recent studies identified that rodent hyalocytes contain macrophage cell surface markers, that these cells are derived from bone marrow, and that they are replaced every 7 months (see chapter II.D. Hyalocytes).

Hyalocytes are embedded in the posterior vitreous cortex (Figures II.E-18 and II.E-19), widely spread apart in a single layer situated 20–50 µm from the inner limiting lamina of the retina posteriorly and the basal lamina of the ciliary body epithelium at the pars plana and vitreous base.

Quantitative studies of cell density in the bovine [113] and rabbit [114] vitreous found the highest density of hyalocytes in the region of the vitreous base, followed next by the posterior pole, with the lowest density at the equator. As shown in Figure II.E-19, hyalocytes are oval or spindle shaped, are 10–15 µm in diameter, and contain a lobulated nucleus, a well-developed Golgi complex, smooth and rough endoplasmic reticula, and many large periodic acid-Schiff-positive lysosomal granules and phagosomes [104, 115]. Hogan and colleagues [116] described that the posterior hyalocytes are flattened and spindle shaped, whereas anterior hyalocytes are larger, rounder, and at times star shaped. Saga and associates [117] have described that different ultrastructural features can be present in different individual cells of the hyalocyte population in an eye. Whether this relates to different origins for the different cells or different states of cell metabolism or activity is not clear.

Balazs [118, 119] pointed out that hyalocytes are located in the region of highest HA concentration and suggested that these cells are responsible for vitreous HA synthesis. In support of this hypothesis is the finding that the enzymes needed for HA synthesis are present within hyalocytes [120]. Osterlin [121] demonstrated that labeled intermediates destined to become incorporated into HA are taken up and internalized by hyalocytes. Several *in vivo* [122, 123] and *in vitro* [123, 124] studies have shown that hyalocytes synthesize large amounts of HA. Bleckmann [125] found that in contrast to *in vivo* metabolism, HA synthesis by hyalocytes grown *in vitro* is reduced in favor of sulfated polysaccharide

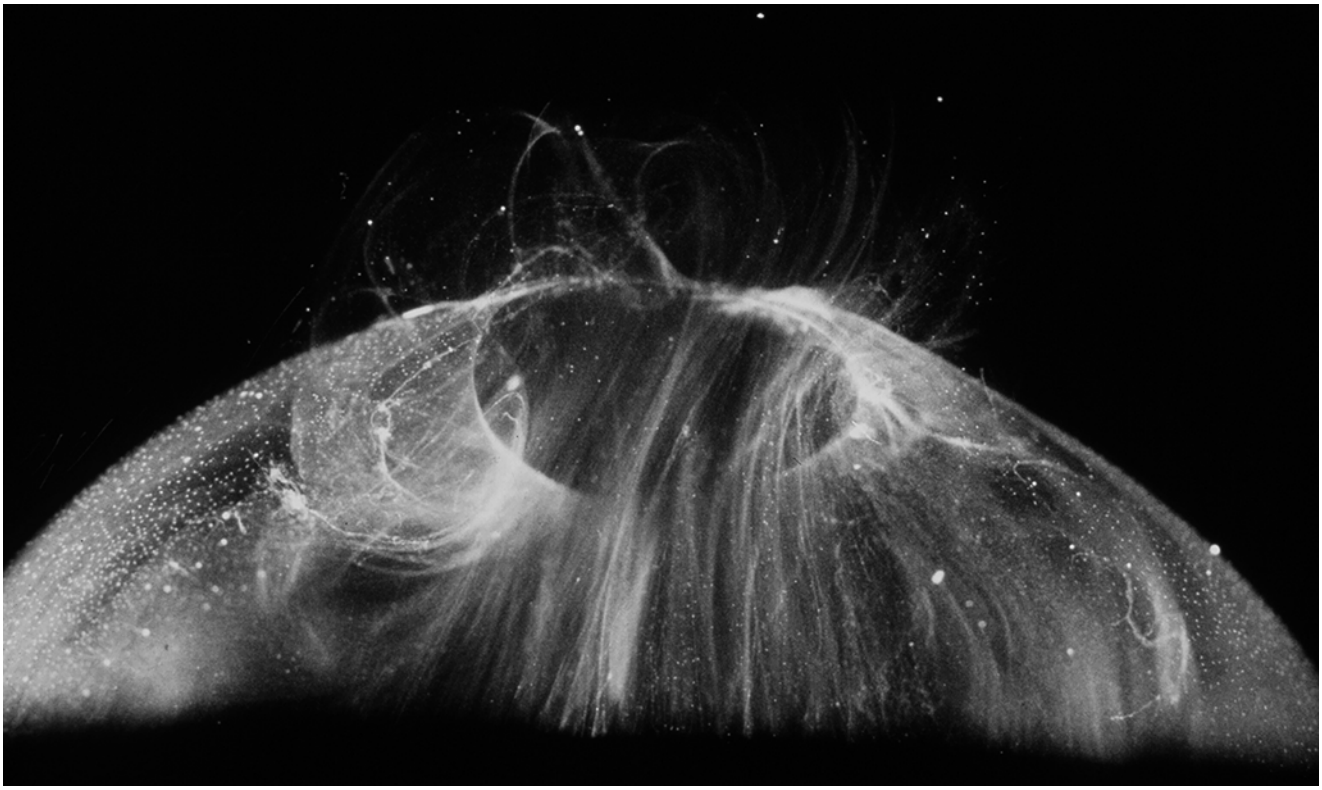

Figure II.E-17 Human posterior vitreous cortex. Posterior vitreous in the left eye of a 59-year-old man. The vitreous cortex envelopes the vitreous body and contains multiple, small points that scatter light intensely, which are mononuclear cells known as hyalocytes. There is a "hole" in the prepapillary posterior vitreous cortex through which vitreous extrudes into the retro-cortical space. Larger amounts of vitreous extrude through the premacular vitreous cortex and fibers course from the central vitreous into the retro-cortical space [108]

synthesis. He suggested that when these cultured cells are reimplanted into vitreous, there must be a retransformation of hyalocyte glycosaminoglycans synthesis to the normal state since vitreous clarity is maintained in these experimental conditions [126]. Swann, however, claimed that there is no evidence that hyalocytes are responsible for the synthesis of vitreous HA. There is no evidence to suggest that hyalocytes maintain ongoing synthesis and metabolism of glycoproteins within the vitreous. Thereafter, Rhodes and coworkers [127] used autoradiography to demonstrate the active incorporation of fucose into rabbit vitreous glycoproteins. In another study [128], sialyl and galactosyl transferase activity was demonstrated in calf vitreous hyalocytes, suggesting that these cells are responsible for vitreous glycoprotein synthesis. An alternate hypothesis, however, states that vitreous glycoproteins originate as secretory products of the inner layer of the ciliary epithelium [129, 130] (see chapter I.F. Vitreous biochemistry and artificial vitreous).

Hyalocyte capacity to synthesize collagen was first demonstrated by Newsome and colleagues [131]. Studies by Ayad and Weiss [132] showed the presence of CPS-1 and CPS-2 collagens adjacent to hyalocytes. These investigators concluded that in similar fashion to chondrocyte metabolism, hyalocytes synthesize these collagens. Hoffman and coworkers [133] also proposed that the distribution of high-molecular-weight substances in vitreous, including enzymes, suggests synthesis by hyalocytes.

The phagocytic capacity of hyalocytes has been described *in vivo* [134] and demonstrated *in vitro* [113, 126]. This activity is consistent with the presence of pinocytic vesicles and phagosomes [114, 135] and the presence of surface receptors that bind IgG and complement [136]. Interestingly, HA may have a regulatory effect on hyalocyte phagocytic activity [137, 138]. Balazs [12] has proposed that in their resting state, hyalocytes synthesize matrix glycosaminoglycans and glycoproteins and that the cells internalize and reuse these macromolecules by way of pinocytosis. In such a state, hyalocytes may prevent cell migration and proliferation, as has been shown for RPE cells and vascular endothelial cells. However, in response to inducting stimuli and inflammation, hyalocytes may become phagocytic as well as stimulatory for monocyte recruitment from the circulation, beginning the cascade of events associated with inflammation and wound repair. This type of transformation may underlie the observations of Saga and associates [117], who identified different appearances in the various cells of a hyalocyte population in a given eye. It is also important to consider that hyalocytes as well as resident fibroblasts are the

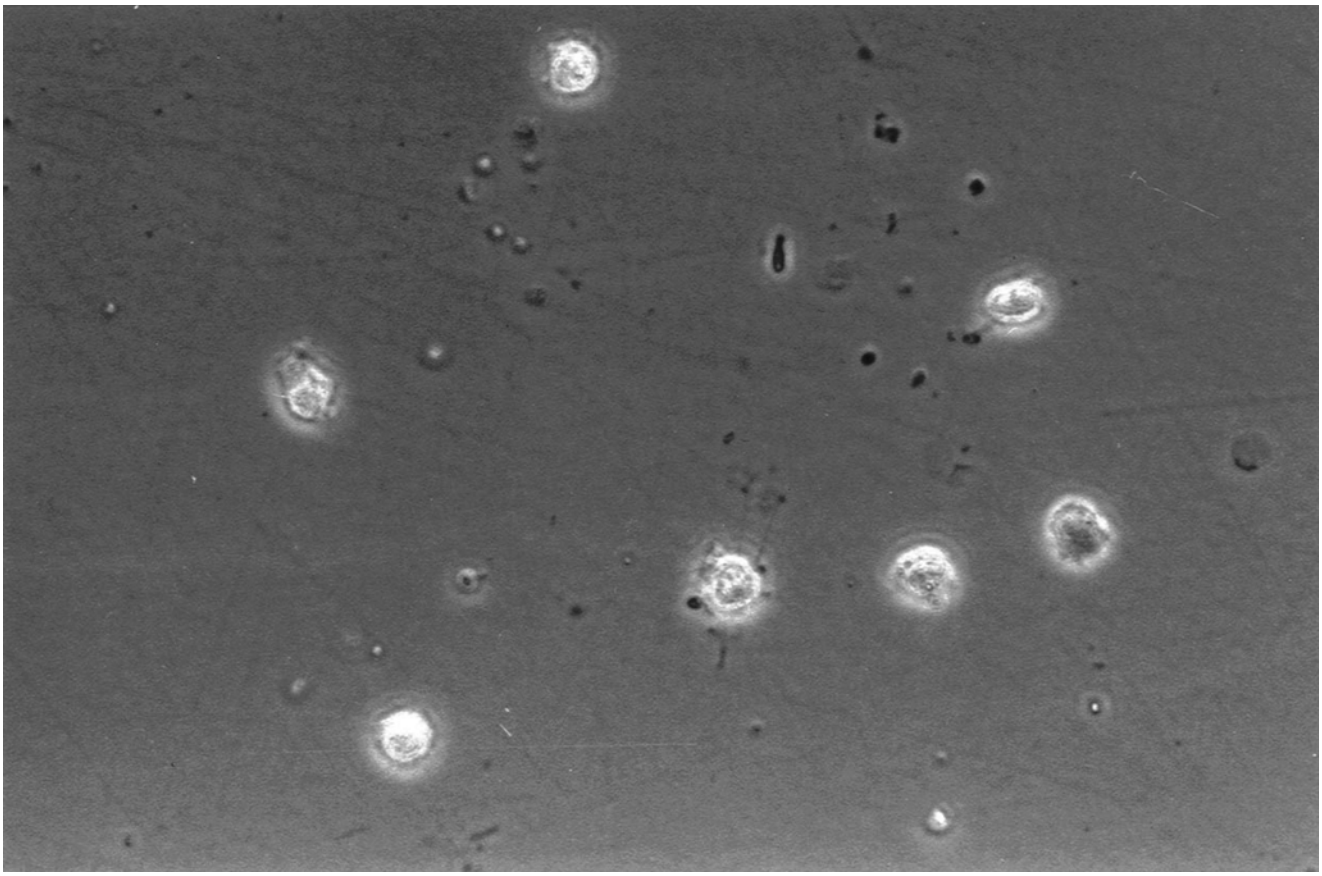

Figure II.E-18 Human hyalocytes *in situ*. Phase contrast microscopy of *in situ* preparation of hyalocytes in the vitreous cortex from the eye of an 11-year-old girl obtained at autopsy. No stains or dyes were used in this preparation. Pseudopodia are visible in some cells (Original magnification = 290×. Specimen courtesy of the New England Eye Bank)

first cells to be exposed to any migratory or mitogenic stimuli. Thus, the response of these cells must be considered in defining the pathophysiology of all proliferative disorders at the vitreoretinal interface, especially PVR and premacular ("epiretinal") membrane formation.

2. Fibroblasts

There is a second population of cells in the vitreous cortex that in some cases may be mistaken for hyalocytes. Several investigations [113, 139, 140] have determined that fibroblasts are present in the vitreous cortex. These cells constitute less than 10 % of the total vitreous cell population and are localized within the vitreous base, adjacent to the ciliary processes and the optic disc. It may be that these cells are involved in vitreous collagen synthesis, especially in pathologic situations. The argument for a role in normal vitreous collagen synthesis is mostly by analogy to studies of fibrillogenesis in tendon where investigators [141] have found that secreted collagen molecules are assembled into fibrils within invaginations of secreting fibroblasts. The locations of fibroblasts in the anterior peripheral vitreous (vitreous base and near the ciliary processes) and posterior vitreous may explain how vitreous fibers become continuous structures spanning the distance between these locations. Balazs and coworkers [113] found that near the pars plana ciliaris, vitreous fibroblasts decrease in number with age. Gartner [139] has suggested that changes in these cells are responsible for aging changes in the collagen network of the vitreous base.

IV. Vitreovascular Interface

While the precise nature of the vitreoretinal interactions in and around retinal blood vessels remains incompletely understood, specialized vitreovascular structures and interrelationships do exist [142]. Kuwabara and Cogan [143] described "spiderlike bodies" in the peripheral retina that coiled about blood vessels and connected with the ILM. Pedler [144] found that the ILM was thin over blood vessels and hypothesized that this was due to the absence of Müller cell inner processes (Figure II.E-20). Wolter [145] noted the existence of pores in the ILM along blood vessels and found vitreous strands inserted where the pores were

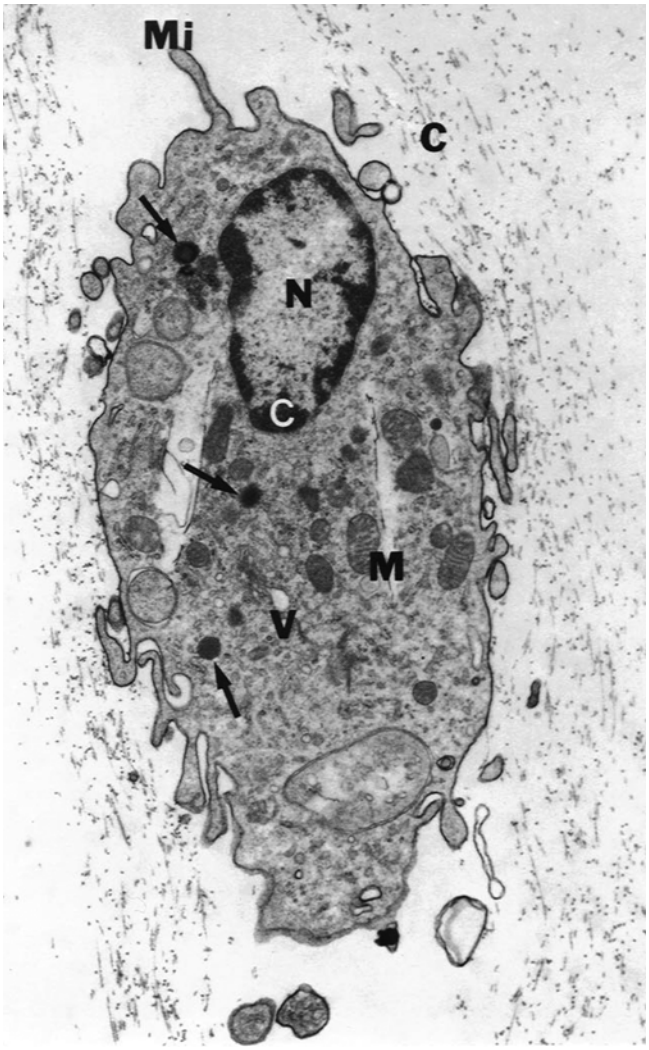

Figure II.E-19 Ultrastructure of human hyalocyte. A mononuclear cell is seen embedded within the dense collagen fibril (*black C*) network of the vitreous cortex. There is a lobulated nucleus (*N*) with dense marginal chromatin (*white C*). In the cytoplasm there are mitochondria (*M*), dense granules (*arrows*), vacuoles (*V*), and microvilli (*Mi*) (×1,670) (Courtesy of JL Craft and DM Albert, Harvard Medical School, Boston) (From Sebag [107])

located. Mutlu and Leopold [146] described these strands as extending through the ILM to branch and surround vessels in what they termed "vitreo-retinal-vascular bands." Such structures might explain the strong adhesion between vitreous and retinal blood vessels, as well as the tendency for vitreous traction to be associated with retinal vascular leakage, retinal neovascularization, and hemorrhage.

Foos [147] proposed a sequence of events in the development of traction associated with retinal blood vessels beginning initially with thinning of the ILM, then subsurface retinal degeneration, and eventually transmigration of macrophages. Small defects in the ILM, when complicated by vitreous incarceration or by simple epiretinal membrane formation can provoke more complex proliferative lesions of the vitreovascular interface. Cystic degeneration occurring along the retinal vessels is present in the nerve fiber layer, is seen before the vitreous is detached at that area, and is referred to as paravascular rarefaction [147–150] (see chapter III.H. Peripheral vitreo-retinal pathology). In a study of eyes of 126 consecutive autopsy cases of subjects 21 years or older at death, Spencer and Foos [148] observed retinal paravascular rarefaction in 30 %. The process was bilateral in 83 % of affected cases and was present in 25 % of the 252 eyes in the study. These paravascular cyts are believed to be a common precursor to both paravascular lamellar retinal tears, also called retinal pits, and many full-thickness retinal tears [148, 149]. This correlation between irregular vitreovascular adherence, paravascular cyst formation, and the development of localized retinal tears has been identified most convincingly in highly myopic eyes [151, 152].

Polk et al. [153] described the clinicopathologic features of a new sheen retinal dystrophy-familial inner limiting membrane dystrophy. Cystic spaces were present under the ILM and in the inner nuclear layer. Numerous areas of separation of the ILM from the retina were present. A filamentous material was present in some of these areas. Endothelial cell swelling and partial degeneration, pericyte degeneration,

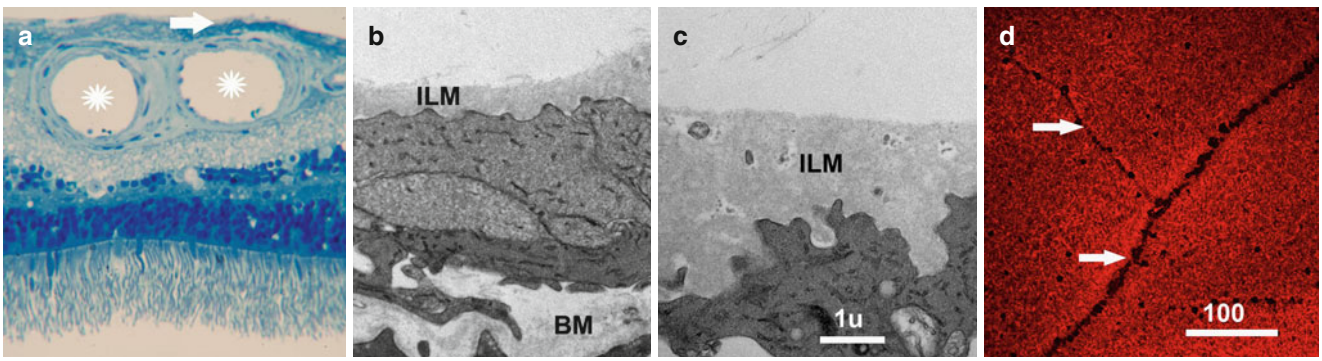

Figure II.E-20 Vitreo-retinal-vascular interface in the human retina. (**a**) Cross section of an 80-year-old human retina with two large vessels (*white stars*) near the ILM. TEM shows that the ILM adjacent to those vessels is thinner (**b**) as compared to the ILM further away from the vessels. *BM* basement membrane of a retinal vessel close to the ILM (**c**). Further, ILM whole mounts stained for laminin show less staining at sites where blood vessels had been in the retina and outline the course of the vessels, confirming that the ILM is thinner when retinal vessels are close to the vitread surface of the retina (**d**) Bars: **b**, **c**: 1um; **d**: 100 um

and basement membrane thickening of retinal capillaries suggested that this condition is primarily a retinal vascular problem with chronic edema, swelling, and degeneration of Müller cells and separation of the ILM.

The risk of hemorrhage is particularly high when abnormal neovascular vessel complexes grow into the posterior vitreous cortex, as shown by Falbourn and Bowald [154]. However, even in the absence of neovascularization, vitreous traction upon retinal vessels can induce vitreous hemorrhage. This can occur in innocuous posterior vitreous detachment (PVD) or in anomalous PVD. Indeed, studies have shown that in nondiabetic patients with fundus-obscuring hemorrhage, there is a 67 % incidence of retinal tears, 39 % with retinal detachment [155]. Traction-mediated avulsion of retinal veins and/or arteries is believed to be an important contributor to the occurrence of vitreous hemorrhage in the absence of new blood vessel formation [see chapter III.H. Peripheral vitreo-retinal pathology].

Irregularities or defects in vitreovascular adherence are common and appear to correspond to areas of cystic degeneration in the nerve fiber layer, also referred to as paravascular rarefraction [147–149]. These paravascular cyts are believed to be a common precursor to both paravascular lamellar retinal tears, also called retinal pits, and many full-thickness retinal tears [147–149]. This correlation between irregular vitreovascular adherence, paravascular cyst formation, and the development of localized retinal tears has been identified most convincingly in highly myopic eyes [151, 152].

V. Unresolved Questions

While the foregoing presents a comprehensive body of information regarding the vitreoretinal interface and particularly the ILM, there are many important questions that remain unresolved.

A. Diffusion Through the ILM

1. Trans-ILM Diffusion from Vitreous to Retina and Choroid

It is currently not known what size particles and proteins can penetrate the ILM. The successful use of avastin, a humanized monoclonal antibody, to treat VEGF-induced subretinal neovascularization in age-related macular degeneration (AMD) shows that antibodies with a molecular weight of 150 kD can penetrate the ILM. Similar experiments in chick embryos also showed that other antibodies could diffuse through the ILM in matter of hours [156]. The upper molecular weight size and the diffusion kinetics, however, are unknown. While peptides and proteins <150 kD can diffuse through BMs, it is unknown whether lipids, lipophilic compounds, and lipoproteins can penetrate the ILM. Another question in this regard relates to the observation that eyes of diabetic patients with vitreoretinal adhesion have a greater risk of having proliferative diabetic retinopathy. One hypothesis is that the vitreoretinal interface in these cases interferes with oxygenation of the inner retina, but there are no studies of trans-ILM oxygen transport/diffusion in diabetics vs. nondiabetics.

2. Trans-ILM Diffusion from Chorioretinal Compartment to Vitreous

Studies have shown that in AMD eyes with vitreomacular adhesion have a higher incidence of choroidal neovascularization than eyes with PVD [157, 158]. One of the hypotheses to explain this observation is that the vitreoretinal interface in these eyes represents a barrier to the egress of proangiogenic cytokines from the chorioretinal compartment. There are no studies that address this possibility.

B. Viral Penetration Through the ILM into the Retina

A convenient way to induce a medically relevant transduction of retinal cells would be an intravitreal injection of virus particles that carry a cDNA to transfect the retinal cells. Preliminary data plating adenoviruses on top of ILM whole mounts showed that these viruses were unable to infiltrate the ILM (Halfter, unpublished). Potential entry sites for viruses are the foveal area, where the ILM is very thin and potentially damaged, and sites with large blood vessels in the nerve fiber layer, where the ILM is also very thin and fragile [153] or segments of the ILM that are damaged. Furthermore, it might be desirable to temporarily alter the integrity of the ILM so as to facilitate viral penetration for therapeutic transfection of the retina.

C. Trans-ILM Cell Migration

The mechanism(s) by which circulating monocytes and retinal glial cells migrate through the ILM to form contractile premacular membranes and cause macular pucker are unknown. Similarly, it is not known how vascular endothelial cells migrate through the ILM to form new blood vessels in ischemic retinopathies such as proliferative diabetic retinopathy.

D. Vitreous-ILM Adhesion

TEM imaging of the vitreoretinal interface showed a connectivity of vitreous ECM proteins and the ILM (Figure II.E-1). The adhesion of both ECM structures is strong in youth. In human eyes from patients before the age

of 30, the vitreous and the ILM are almost inseparable and make vitrectomy problematic. Further, high myopia lead to PVD at a relative early age and may cause retinal detachment. This happens at a high frequency in Knobloch syndrome patients, where high myopia lead to a precocious and consequently anomalous PVD followed by giant retinal detachments.

Russell [159] proposes a model by which the ECM maintains integrity of the vitreoretinal interface. In his theory, a 240 kDa protein core is bound to the type IV collagen of the ILM. Attached to the protein core are series of chondroitin sulfate glycosaminoglycans (GAG) that are present on the vitread side of the ILM. The GAGs bind to a fibrillar protein, most likely opticin, which then interacts with type II collagen of the cortical vitreous. Through this chain of interaction, ILM to core protein to GAG to opticin to cortical vitreous, a relatively strong biochemical adhesion is formed. The adhesion of vitreous and ILM becomes progressively weaker with advancing age, and at the age of 60 and older, the vitreous separates by itself from the ILM during posterior vitreous detachment (PVD). What is currently unknown is what molecular partners in ILM and vitreous connect both structures. Since this connectivity is most likely the cause for retinal tears and other pathologies during anomalous PVD, it would be important to have a better understanding of the molecular partners that provide the junction between the vitreous and the ILM.

Abbreviations

AFM	Atomic force microscopy
AMD	Age-related macular degeneration
BM	Basement membrane
GAG	Glycosaminoglycans
IgG	Immunoglobulin G
ILM	Inner limiting membrane
kD	Kilodalton
PBS	Phosphate-buffered saline
PVD	Posterior vitreous detachment
PVR	Proliferative vitreoretinopathy
TEM	Transmission electron microscopy
VEGF	Vascular endothelial growth factor

References

1. Salzmann as cited by Hogan MJ, Alvarado JA, Weddel JE. Histology of the human eye: an atlas and textbook. Philadelphia: WB Saunders; 1971. 488 p.
2. Heegaard S. Morphology of the vitreoretinal border region. Acta Ophthalmol Scand Suppl. 1997;222:1–31.
3. Candiello J, Balasubramani M, Schreiber EM, Cole GJ, Mayer U, Halfter W, et al. Biomechanical properties of native basement membranes. FEBS J. 2007;274:2897–908. PMID: 17488283.
4. Candiello J, Cole GJ, Halfter W. Age-dependent changes in the structure, composition and biophysical properties of a human basement membrane. Matrix Biol. 2010;29:402–10. PMID: 20362054.
5. Binning G, Quate CF, Gerber C. Atomic force microscope. Phys Rev Lett. 1986;56:930–3. PMID: 10033323.
6. Laney DE, Garcia RA, Parsons SM, Hansma HG. Changes in the elastic properties of cholinergic synaptic vesicles as measured by atomic force microscopy. Biophys J. 1997;72:806–13. PMID: 9017205.
7. A-Hassan E, Heinz WF, Antonik MD, D'Costa NP, Nageswaran S, Schoenenberger CA, et al. Relative microelastic mapping of living cells by atomic force microscopy. Biophys J. 1998;74:1564–78. PMID: 9512052.
8. Quist AP, Rhee SK, Lin H, Lal R. Physiological role of gap-junctional hemichannels. Extracellular calcium-dependent isosmotic volume regulation. J Cell Biol. 2000;148:1063–74. PMID: 10704454.
9. Loparic M, Wirz D, Daniels AU, Raiteri R, Vanlandingham MR, Guex G, et al. Micro- and nanomechanical analysis of articular cartilage by indentation-type atomic force microscopy: validation with a gel-microfiber composite. Biophys J. 2010;98:2731–40. PMID: 20513418.
10. Danysh BP, Czymmek KJ, Olurin PT, Sivak JG, Duncan MK. Contributions of mouse genetic background and age o anterior lens capsule thickness. Anat Rec. 2008;291:1619–27. PMCID: PMC2699617.
11. Kiani C, Chen L, Wu YJ, Yee AJ, Yang BB. Structure and function of aggrecan. Cell Res. 2002;12:19–32.
12. Balazs EA. Functional anatomy of the vitreous. In: Duane TD, Jaeger EA, editors. Biomedical foundations of ophthalmology. Philadelphia: JB Lippincott; 1984.
13. Balasubramani M, Schreiber EM, Candiello J, Balasubramani GK, Kurtz J, Halfter W. Molecular interactions in the retinal basement membrane system: a proteomic approach. Matrix Biol. 2010;29:471–83. PMID: 20403434.
14. Heergaard S, Jensen OA, Prause JU. Structure of the vitread face of the monkey optic disc (Macaca mulatta): SEM on frozen resin-cracked optic nerve heads supplemented by TEM and immunohistochemistry. Graefes Arch Clin Exp Ophthalmol. 1988;226:377.
15. Henrich PB, Monnier CA, Halfter W, Haritoglou C, Strauss RW, Lim RY, et al. Nanoscale topographic and biomechanical studies of the human internal limiting membrane. Invest Ophthalmol Vis Sci. 2012;53:2561–70. PMID: 22410559.
16. Foos RY. Posterior vitreous detachment. Trans Am Acad Ophthalmol Otolaryngol. 1972;76:480.
17. Foos RY. Vitreoretinal juncture over retinal vessels. Albrecht Von Graefes Arch Klin Exp Ophthalmol. 1977;204:223–34. PMID: 304681.
18. Chung AE, Freeman IL, Braginski JE. A novel extracellular membrane elaborated by a mouse embryonal carcinoma-derived cell line. Biochem Biophys Res Commun. 1977;79:859–68. PMID: 597311.
19. Chung AE. Embryonal carcinoma and the basement membrane glycoproteins laminin and entactin. Int J Dev Biol. 1993;37:141–50. PMID: 8507559.
20. Kleinman HK, Martin GR. Matrigel: basement membrane matrix with biological activity. Semin Cancer Biol. 2005;15:378–86. PMID: 15975825.
21. Chung AE, Jaffe R, Freeman IL, Vergnes JP, Braginski JE, Carlin B. Properties of a basement membrane-related glycoprotein synthesized in culture by a mouse embryonal carcinoma-derived cell line. Cell. 1979;16:277–87. PMID: 88263.
22. Timpl R, Rohde H, Robey PG, Rennard SI, Foidart JM, Martin GR. Laminin – a glycoprotein from basement membranes. J Biol Chem. 1979;254:9933–7. PMID: 114518.
23. Carlin B, Jaffe R, Bender B, Chung AE. Entactin, a novel basal lamina-associated sulfate glycoprotein. J Biol Chem. 1981;256:5209–14. PMID: 6262321.

24. Timpl R, Dziadek M, Fujiwara S, Nowack H, Wick G. Nidogen: a new self-aggregating basement membrane protein. Eur J Biochem. 1983;137:455–65. PMID: 6420150.
25. Hassell JR, Robey PG, Barrach HJ, Wilczek J, Rennard SI, Martin GR. Isolation of a heparan sulfate-containing proteoglycan from basement membrane. Proc Natl Acad Sci. 1980;77:4494–8.
26. Kleinman HK, McGarvey ML, Liotta LA, Robey PG, Tryggvason K, Martin GR. Isolation and characterization of type IV procollagen, laminin, and heparan sulfate proteoglycan from the EHS sarcoma. Biochemistry. 1982;21:6188–93.
27. Paulsson M, Aumailley M, Deutzmann R, Timpl R, Beck K, Engel J. Laminin-nidogen complex. Extraction with chelating agents and structural characterization. Eur J Biochem. 1987;166:11–9. PMID: 3109910.
28. Timpl R, Brown JC. Supramolecular assembly of basement membranes. Bioassays. 1996;18:123–32. PMID: 8851045.
29. Erickson AC, Couchman JR. Still more complexity in mammalian basement membranes. J Histochem Cytochem. 2000;48:1291–306. PMID: 10990484.
30. Miner JH, Yurchenco PD. Laminin functions in tissue morphogenesis. Annu Rev Cell Dev Biol. 2004;20:255–84. PMID: 15473841.
31. Hohenester E, Yurchenco PD. Laminins in basement membrane assembly. Cell Adh Migr. 2013;7:56–63. PMID: 23076216.
32. Khoshnoodi J, Pedchenko V, Hudson BG. Mammalian collagen IV. Microsc Res Tech. 2008;71:357–70.
33. Ho MS, Böse K, Mokkapati S, Nischt R, Smyth N. Nidogens-extracellular matrix linker molecules. Microsc Res Tech. 2008;71: 387–95. PMID: 18219668.
34. Iozzo RV. Basement membrane proteoglycans: from cellar to ceiling. Ant Rev Mol Cell Biol. 2005;6:646–56. PMID: 16064139.
35. Ljubimov AV, Burgeson RE, Butkowski RJ, Couchman JR, Zardi L, Ninomiya Y, et al. Basement membrane abnormalities in human eyes with diabetic retinopathy. J Histochem Cytochem. 1996;44: 1469–79. PMID: 8985139.
36. Libby RT, Champliaud M-F, Claudepierre T, Xu Y, Gibbons EP, Koch M, et al. Laminin expression in adult and developing retinae: evidence of two novel CNS laminins. J Neurosci. 2000;20:6517–28. PMID: 10964957.
37. Uechi G, Sun Z, Schreiber E, Halfter W, Balasubramani M. A proteomic view of basement membranes from human retinal blood vessels, inner limiting membranes and lens capsules. J Proteomic Res. [in press]
38. Balazs EA. The vitreous. Int Ophthalmol Clin. 1973;15:53–63.
39. Timpl R, Wiedemann H, van Delden V, Furthmayr H, Kuehn K. A network model for the organization of type IV collagen molecules in basement membranes. Eur J Biochem. 1981;120:203–11. PMID: 6274634.
40. Schittny JC, Timpl R, Engel J. High resolution immunoelectron microscopic localization of functional domains of laminin, nidogen, and heparan sulfate proteoglycan in epithelial basement membrane of mouse cornea reveals different topological orientations. J Cell Biol. 1988;107:1599–610. PMID: 2459133.
41. Yurchenco PD, Ruben GC. Basement membrane structure in situ: evidence for lateral associations in the type IV collagen network. J Cell Biol. 1987;105:2559–68. PMID: 3693393.
42. Fox JW, Mayer U, Nischt R, Aumailley M, Reinhardt D, Wiedemann H, et al. Recombinant nidogen consists of three globular domains and mediates binding of laminin to collagen type IV. EMBO J. 1991;10:3137–46. PMID: 1717261.
43. Yurchenco PD, Patton BL. Developmental and pathogenic mechanisms of basement membrane assembly. Curr Pharm Des. 2009;15:1277–94.
44. Murshed M, Smyth N, Miosge N, Karolat J, Krieg T, Paulsson M, et al. The absence of nidogen 1 does not affect murine basement membrane formation. Mol Cell Biol. 2000;20:7007–12. PMID: 10958695.
45. Bader BL, Smyth N, Nedbal S, Miosge N, Baranowsky A, Mokkapati S, et al. Compound genetic ablation of nidogen 1 and 2 causes basement membrane defects and perinatal lethality in mice. Mol Cell Biol. 2005;25:6846–56.
46. Grant DS, Leblond CP, Kleinman HK, Inoue S, Hassell JR. The incubation of laminin, collagen IV, and heparan sulfate proteoglycan at 35 degrees C yields basement membrane-like structures. J Cell Biol. 1989;108:1567–74.
47. Stephens LE, Sutherland AE, Klimanskaya IV, Andrieux A, Meneses J, Pedersen RA, et al. Deletion of beta 1 integrins in mice results in inner cell mass failure and peri-implantation lethality. Genes Dev. 1995;9:1883–95. PMID: 7544312.
48. Henry MD, Campbell KP. A role for dystroglycan in basement membrane assembly. Cell. 1998;95:859–70. PMID: 9865703.
49. Dong LJ, Chung AE. The expression of genes for entactin, laminin A, laminin B1 and laminin B2 in murine lens morphogenesis and eye development. Differentiation. 1991;48:157–72. PMID: 1725162.
50. Halfter W, Dong S, Schurer B, Osanger A, Schneider W, Ruegg M, et al. Composition, synthesis, and assembly of the embryonic chick retinal basal lamina. Dev Biol. 2000;220:111–28. PMID: 10753504.
51. Dong L, Chen Y, Lewis M, Hsieh JC, Reing J, Chaillet JR, Howell CY, Melhem M, Inoue S, Kuszak JR, DeGeest K, Chung AE. Neurological defects and selective disruption of basement membranes in mice lacking entactin-1/nidogen-1. Lab Invest. 2002;82:1617–30. PMID: 12480912.
52. Halfter W, Willem M, Mayer U. Basement membrane-dependent survival of retinal ganglion cells. Invest Ophthalmol Vis Sci. 2005;46:1000–9.
53. Halfter W, Dong S, Schurer B, Ring C, Cole GJ, Eller A. Embryonic synthesis of the inner limiting membrane and vitreous body. Invest Ophthalmol Vis Sci. 2005;46:2202–9. PMID: 15914642.
54. Sarthy V, Collagen IV. mRNA expression during development of the mouse retina: an in situ hybridization study. Invest Ophthalmol Vis Sci. 1993;34:145–52. PMID: 7678834.
55. Halfter W, Dong S, Dong A, Eller AW, Nischt R. Origin and turnover of ECM proteins from the inner limiting membrane and vitreous body. Eye (Lond). 2008;22:1207–13. PMID: 18344966.
56. Foos RY, Gloor BP. Vitreoretinal juncture; healing of experimental wounds. Albrecht Von Graefes Arch Klin Exp Ophthalmol. 1975; 196:213–20.
57. Ponsioen TL, van Luyn MJA, van der Worp RJ, Pas HH, Hooymans JMM, Los LI. Human retinal Müller cells synthesize collagens of the vitreous and vitreo-retinal interface *in vitro*. Mol Vis. 2008;14:652–60.
58. Nakamura T, Murata T, Hisatomi T, Enaida H, Sassa Y, Ueno A, et al. Ultrastructure of the vitreoretinal interface following the removal of the internal limiting membrane using indocyanine green. Curr Eye Res. 2003;27(6):395–9.
59. Sebag J, Hageman GS. Interfaces. Eur J Ophthalmol. 2000;10: 1–3.
60. Sebag J, Hageman GS. Interfaces. Fondazione GB Bietti Per lo Studio e la Ricerca in Oftalmologia. Roma: Farina Publishers; 2000.
61. Lee J, Gross JM. Laminin beta1 and gamma1 containing laminins are essential for basement membrane integrity in the zebrafish eye. Invest Ophthalmol Vis Sci. 2007;48:2483–90.
62. Edwards MM, Mammadova-Bach E, Alpy F, Klein A, Hicks WL, Roux M, et al. Mutations in Lama1 disrupt retinal vascular development and inner limiting membrane formation. J Biol Chem. 2010;285(10):7697–711.
63. Pinzón-Duarte G, Daly G, Li YN, Koch M, Brunken WJ. Defective formation of the inner limiting membrane in laminin beta2-and gamma3-null mice produces retinal dysplasia. Invest Ophthalmol Vis Sci. 2010;51:1773–82. PMID: 19907020.
64. Labelle-Dumais C, Dilworth DJ, Harrington EP, de Leau M, Lyons D, Kabaeva Z, et al. COL4A1 mutations cause ocular dysgenesis, neural localization defects, myopathy in mice and Walker-Warburg syndrome in humans. PLoS Genet. 2011;7: e1002062. PMID: 21625620.

65. Takeda S, Kondo M, Sasaki J, Kurahashi H, Kano H, Arai K, et al. Fukutin is required for maintenance of muscle integrity, cortical histiogenesis and normal eye development. Hum Mol Genet. 2003;12:1449–59. PMID: 12783852.
66. Lee Y, Kameya S, Cox GA, Hsu J, Hicks W, Maddatu TP, Smith RS, Naggert JK, Peachey NS, Nishina PM. Ocular abnormalities in Large (myd) and Large (vls) mice, spontaneous models for muscle, eye, and brain diseases. Mol Cell Neurosci. 2005;30:160–72.
67. Hu H, Candiello J, Zhang P, Ball SL, Cameron DA, Halfter W. Retinal ectopias and mechanically weakened basement membrane in a mouse model of muscle-eye-brain (MEB) disease congenital muscular dystrophy. Mol Vis. 2010;16:1415–28. PMID: 20680099.
68. Silan F, Yoshioka M, Kobayashi K, Simsek E, Tunc M, Alper M, et al. A new mutation of the fukutin gene in a non-Japanese patient. Ann Neurol. 2003;53:392–6.
69. Beltra´n-Valero de Bernabe D, van Bokhoven H, van Beusekom E, Van den Akker W, Kant S, Dobyns B, et al. A homozygous nonsense mutation of the Fukutin gene causes a Walker-Warburg Syndrome phenotype. J Med Genet. 2003;40:845–8.
70. Taniguchi K, Kobayashi K, Saito K, Yamanouchi H, Ohnuma A, Hayashi YK, et al. Distribution and broader clinical spectrum of muscle-eye-brain disease. Hum Mol Genet. 2003;12:527–34.
71. Clement E, Mercuri E, Godfrey C, Smith J, Robb S, Kinali M, Straub V, Bushby K, Manzur A, Talim B, Cowan F, Quinlivan R, Klein A, Longman C, McWilliam R, Topaloglu H, Mein R, Abbs S, North K, Barkovic J, Rutherford M, Muntoni F. Brain involvement in muscular dystrophies with defective dystroglycan glycosylation. Ann Neurol. 2008;64:573–82.
72. Halfter W, Dong S, Yip YP, Willem M, Mayer U. A critical function of the pial basement membrane in cortical histogenesis. J Neurosci. 2002;22:6029–40.
73. Gould DB, Phalan FC, Breedveld GJ, van Mil SE, Smith RS, Schimenti JC, et al. Mutations in Col4A1 cause perinatal cerebral hemorrhage and porencephaly. Science. 2005;308:1167–71.
74. Muntoni F, Torelli S, Brockington M. Muscular dystrophies due to glycosylation defects. Neurotherapeutics. 2008;5:627–32.
75. Matsumoto B, Blanks JC, Ryan SJ. Topographic variations in the rabbit and primate internal limiting membrane. Invest Ophthalmol Vis Sci. 1984;1:71–82.
76. Sebag J, Buckingham B, Charles MA, Reiser K. Biochemical abnormalities in vitreous of humans with proliferative diabetic retinopathy. Arch Ophthalmol. 1992;110:1472–9.
77. Sebag J, Nie S, Reiser KA, Charles MA, Yu NT. Raman spectroscopy of human vitreous in proliferative diabetic retinopathy. Invest Ophthalmol Vis Sci. 1994;35:2976–80.
78. Sebag J. Abnormalities of human vitreous structure in diabetes. Graefes Arch Clin Exp Ophthalmol. 1993;231:257–60.
79. Sebag J. Diabetic vitreopathy. Ophthalmology. 1996;103:205–6.
80. Matsunaga N, Ozeki H, Hirabayashi Y, Shimada S, Ogura Y. Histopathological evaluation of the inner limiting membrane surgically excised from eyes with diabetic maculopathy. Retina. 2005;25:311–6. PMID: 15805908.
81. Tamura K, Yokoyama T, Ebihara N, Murakami A. Histopathologic analysis of the internal limiting membrane surgically peeled from eyes with diffuse diabetic macular edema. Jpn J Ophthalmol. 2012; 56:280–7. PMID: 22438196.
82. To M, Goz M, Camenzind L, Oertle P, Candiello J, Sullivan M, Henrich PB, Loparic M, Safi F, Eller A, Halfter W. Diabetes-induced morphological, biomechanical and compositional changes of ocular basement membranes. Exp Eye Res. 2013;116:298–307.
83. Abari E, Kociok N, Hartman U, Semkova I, Paulsson M, Lo A, et al. Alterations in basement membrane immunoreactivity of the diabetic retina in three diabetic mouse models. Graefes Arch Clin Exp Ophthalmol. 2013;251:763–75.
84. Roy S, Maiello M, Lorenzi M. Increased expression of basement membrane collagen in human diabetic retinopathy. J Clin Invest. 1994;93:38–442.
85. Sebag J. Anomalous PVD, – a unifying concept in vitreo-retinal diseases. Graefes Arch Clin Exp Ophthalmol. 2004;242:690–8.
86. Sebag J. Vitreous anatomy, aging, and anomalous posterior vitreous detachment. In: Dartt DA, Besharse JC, Dana R, editors. Encyclopedia of the eye, vol. 4. Oxford: Elsevier; 2010. p. 307–15.
87. Sebag J, Gupta P, Rosen R, Garcia P, Sadun AA. Macular holes and macular pucker: the role of vitreoschisis as imaged by optical coherence tomography/scanning laser ophthalmoscopy. Trans Am Ophthalmol Soc. 2007;105:121–31.
88. Sebag J. Vitreoschisis. Graefes Arch Clin Exp Ophthalmol. 2008;246:329–32.
89. Sebag J. Vitreoschisis in diabetic macular edema. Invest Ophthalmol Vis Sci. 2011;52(11):8455–6.
90. Gupta P, Yee KMP, Garcia P, Rosen RB, Parikh J, Hageman GS, et al. Vitreoschisis in macular diseases. Br J Ophthalmol. 2011; 95(3):376–80.
91. Yurchenco PD. Basement membranes: cell scaffoldings and signaling platforms. Cold Spring Harb Perspect Biol. 2011;3.
92. Edwards MM, Lefebvre O. Laminins and retinal vascular development. Cell Adh Migr. 2013;7(1):82–9.
93. Loparic M, Henrich PB. The bi-functional organization of human basement membranes. PLoS One. 2013;8:e67660. PMID: 23844050.
94. Gass JDM. Vitreous maculopathies. In: Stereoscopic atlas of macular diseases. St Louis: Mosby; 1987. p. 676–713.
95. Meezan E, Hjelle JT, Brendel K, Carlson EC. A simple, versatile, nondisruptive method for the isolation of morphologically and chemically pure basement membranes from several tissues. Life Sci. 1975;17:1721–32. PMID: 1207385.
96. Duhamel RC, Meezan E, Brendel K. Selective solubilization of two populations of polypeptides from bovine retinal basement membranes. Exp Eye Res. 1983;36:257–67. PMID: 6297940.
97. Halfter W, Candiello J, Hu H, Zhang P, Schreiber E, Balasubramani M. Protein composition and biomechanical properties of in vivo-derived basement membranes. Cell Adh Migr. 2013;7:64–71. PMID: 23154404.
98. Janmey PA, McCulloch CA. Cell mechanics: integrating cell responses to mechanical stimuli. Annu Rev Biomed Eng. 2007;9: 1–34. PMID: 17461730.
99. Ossewaarde-van Norel A, Rothova A. Imaging methods for inflammatory macular edema. Int Ophthal Clin. 2012;52(4):55–66.
100. Onal S, Tugal-Tutkun I, Neri P, Herbort CP. Optical coherence tomography imaging in uveitis. Int Ophthalmol. 2013;34(2):401–35.
101. Nussenblatt RB. Macular alterations secondary to intraocular inflammatory disease. Ophthalmology. 1986;93:984–8.
102. Bonnin N, Cornut PL, Chaise F, Labeille E, Manificat HJ, Feldman A, et al. Spontaneous closure of macular holes secondary to posterior uveitis: case series and a literature review. J Ophthalmic Inflamm Infect. 2013;3(1):34–40.
103. Sullu Y, Sariaydin G, Kuruoglu S, Bened U. Widespread vitreoretinal traction simulating retinal vasculitis in a patient with uveitis. Retin Cases Brief Rep. 2012;6:379–82.
104. Streeten BA. Disorders of the vitreous. In: Garner A, Klintworth GK, editors. Pathobiology of ocular disease – a dynamic approach, part B, chap 49. New York: Marcel Dekker; 1982. p. 1381–419.
105. Balazs EA. Molecular morphology of the vitreous body. In: Smelser GK, editor. The structure of the eye. New York: Academic; 1961. p. 293–310.
106. Theopold H, Faulborn J. Scanning electron microscopic aspects of the vitreous body. Mod Probl Ophthalmol. 1979;20:92.
107. Sebag J. The vitreous–structure, function and pathobiology. New York: Springer; 1989.
108. Sebag J, Balazs EA. Human vitreous fibres and vitreoretinal disease. Trans Ophthalmol Soc U K. 1985;104:123.
109. Reeser FH, Aaberg T. Vitreous humor. In: Records PE, editor. Physiology of the human eye and visual system. Hagerstown: Harper & Row; 1979. p. 1–31.

110. Schwalbe G. In: Engelmann W, editor. Von Graefe–Saemisch's Handbuch der Gesamnten Augenheilkunde, vol 1. Leipzig; 1874. P. 457.
111. Schwalbe G. Lehrbuch der Anatomie des Auges. Erlangen: E Besold; 1887. p. 288.
112. Balazs EA. In: Acta XVIII. Concilium ophthalmologicum, vol 2. Brussels: 1958. p. 1296.
113. Balazs EA, Toth LZ, Eckl EA, Mitchell AP. Studies on the structure of the vitreous body: XII. Cytological and histochemical studies on the cortical tissue layer. Exp Eye Res. 1964;3:57.
114. Gloor BP. Cellular proliferation on the vitreous surface after photocoagulation. Graefes Arch Clin Exp Ophthalmol. 1969;178:99.
115. Bloom GD, Balazs EA. An electron microscope study of hyalocytes. Exp Eye Res. 1965;4:249.
116. Hogan MJ, Alvarado JA, Weddel JE. Histology of the human eye: an atlas and textbook. Philadelphia: WB Saunders; 1971. p. 607.
117. Saga T, Tagawa Y, Takeuchi T, et al. Electron microscopic study of cells in vitreous of guinea pig. Jpn J Ophthalmol. 1984;28:239.
118. Balazs EA. Structure of vitreous gel. In: Acta XVII concilium ophthalmologicum, vol. 11. 1954. p. 1019.
119. Balazs EA. Studies on structure of vitreous body: absorption of ultraviolet light. Am J Ophthalmol. 1954;38:21.
120. Jacobson B, Osterlin S, Balazs EA. A soluble hyaluronic acid synthesizing system from calf vitreous. Proc Fed Am Soc Exp Biol. 1966;25:588.
121. Osterlin SE. The synthesis of hyaluronic acid in the vitreous. III. In vivo metabolism in the owl monkey. Exp Eye Res. 1968;7:524.
122. Osterlin SE. The synthesis of hyaluronic acid in the vitreous: IV. Regeneration in the owl monkey. Exp Eye Res. 1969;8:27.
123. Berman ER, Gambos GM. Studies on the incorporation of U-14 C-glucose into vitreous polymers *in vitro* and *in vivo*. Invest Ophthalmol. 1969;18:521.
124. Balazs EA, Sundblad L, Toth LZJ. *In vitro* formation of hyaluronic acid by cells in the vitreous body and by lamb tissue. Abstr Fed Proc. 1958;17:184.
125. Bleckmann H. Glycosaminoglycan metabolism of cultured fibroblasts from bovine vitreous. Graefes Arch Clin Exp Ophthalmol. 1984;222:90.
126. François J, Victoria-Troncoso V, Maudgal PC. Immunology of the vitreous body. Mod Probl Ophthalmol. 1976;16:196.
127. Rhodes RH, Mandelbaum SH, Minckler DS, Cleary PE. Tritiated fucose incorporation in the vitreous body, lens and zonules of the pigmented rabbit. Exp Eye Res. 1982;34:921.
128. Jacobson B. Degradation of glycosaminoglycans by extracts of calf vitreous hyalocytes. Exp Eye Res. 1984;39:373.
129. Haddad A, Almeida JC, Laicine EM, et al. The origin of the intrinsic glycoproteins of the rabbit vitreous body: an immunohistochemical and autoradiographic study. Exp Eye Res. 1990;50:555.
130. Haddad A, Laicine EM. Studies on the origin of the glycoproteins of the rabbit vitreous body using a protein synthesis inhibitor and radioactive fucose and amino acids. Germ J Ophthalmol. 1993;2:127.
131. Newsome DA, Linsemayer TF, Trelstad RJ. Vitreous body collagen: evidence for a dual origin from the neural retina and hyalocytes. J Cell Biol. 1976;71:59.
132. Ayad S, Weiss JB. A new look at vitreous humour collagen. Biochem J. 1984;218:835.
133. Hoffmann K, Baurwieg H, Riese K. Uber Gehalt und Vertailang niederund hoch molekularer Substanzen in Glaskorper: II. Hoch molekulare Substanzen (LDH, MDH, GOT). Graefes Arch Clin Exp Ophthalmol. 1974;191:231.
134. Teng CC. An electron microscopic study of cells in the vitreous of the rabbit eye: I. The macrophage. Eye Ear Nose Throat Month. 1969;48:91.
135. Freeman MI, Jacobson B, Toth LZ, Balazs EA. Lysosomal enzymes associated with hyalocyte granules: I. Intercellular distribution patterns of enzymes. Exp Eye Res. 1968;7:113.
136. Grabner G, Baltz G, Forster O. Macrophage-like properties of human hyalocytes. Invest Ophthalmol Vis Sci. 1980;19:333.
137. Forrester JV, Balazs EA. Inhibition of phagocytosis by high molecular weight hyaluronate. Immunology. 1980;40:435.
138. Sebag J, Balazs EA, Eakins KE, Kulkarni P. The effect of Na-hyaluronate on prostaglandin synthesis and phagocytosis by mononuclear phagocytes. Invest Ophthalmol Vis Sci. 1981;20:33.
139. Gartner J. Electron microscopic study on the fibrillar network and fibrocyte-collagen interactions in the vitreous cortex at the ora serrata of human eyes with special regard to the role of disintegrating cells. Exp Eye Res. 1986;42:21.
140. Fine BS, Tousimis AJ. The structure of the vitreous body and the suspensory ligaments of the lens. Arch Ophthalmol. 1961;65:95,119.
141. Birck DE, Zychard EI. Collagen fibrillogenesis *in situ*: fibril segments are intermediates in matrix assembly. Proc Natl Acad Sci U S A. 1989;86:4549.
142. Gloor BP, Daicker BC. Pathology of the vitreo-retinal border structures. Trans Ophthalmol Soc U K. 1975;95:387.
143. Kuwabara T, Cogan DG. Studies of retinal vascular patterns: I. Normal architecture. Arch Ophthalmol. 1960;64:904.
144. Pedler C. The inner limiting membrane of the retina. Br J Ophthalmol. 1961;45:423.
145. Wolter JR. Pores in the internal limiting membrane of the human retina. Acta Ophthalmol. 1964;42:971.
146. Mutlu F, Leopold IH. Structure of the human retinal vascular system. Arch Ophthalmol. 1964;71:93.
147. Foos RY. Vitreo-retinal juncture over retinal vessels. Graefes Arch Clin Exp Ophthalmol. 1977;204:223–34.
148. Spencer LM, Foos RY. Paravascular vitreoretinal attachments: role in retinal tears. Arch Ophthalmol. 1970;84:557–64.
149. Sebag J, Green WR. Vitreous and vitreo-retinal interface. In: Ryan SJ, editor. Retina. Philadelphia: Elsevier; 2012.
150. Sebag J. Vitreoretinal interface and the role of vitreous in macular disease. In: Brancato R, Coscasa G, Lumbrosos B, editors. Proceedings of the retina workshop. Amsterdam: Kugler & Ghedini; 1987. p. 3–6.
151. Hayashi W, Shimada N, Hayashi K, Moriyama M, Yoshida T, Tokoro T, et al. Retinal vessels and high myopia. Ophthalmology. 2011;118(4):791.
152. Komeima K, Kikuchi M, Ito Y, Terasaki H, Miyake Y. Paravascular inner retinal cleavage in a highly myopic eye. Arch Ophthalmol. 2005;123(10):1449–50.
153. Polk TD, Gass DM, Green WR, et al. Familial internal limiting membrane dystrophy: a new sheen retinal dystrophy. Arch Ophthalmol. 1997;115:878–85.
154. Faulborn J, Bowald S. Microproliferations in proliferative diabetic retinopathy and their relationship to the vitreous: corresponding light and electron microscopic studies. Graefes Arch Clin Exp Ophthalmol. 1985;223(3):130–8.
155. Sarrafizadeh R, Hassan TS, Ruby AJ, Williams GA, Garretson BR, Capone Jr A, Trese MT, Margherio RR. Incidence of retinal detachment and visual outcome in eyes presenting with posterior vitreous separation and dense fundus-obscuring vitreous hemorrhage. Ophthalmology. 2001;108(12):2273–8.
156. Halfter W, Winzen U, Bishop PN, Eller A. Regulation of eye size by retinal basement membrane and vitreous body. Invest Ophthalmol Vis Sci. 2006;47:3586–94. PMID: 16877433.
157. Krebs I, Brannath W, Glittenberg K, Zeiler F, Sebag J, Binder S. Posterior vitreo-macular adhesion: a potential risk factor for exudative age-related macular degeneration. Am J Ophthalmol. 2007;144:741–6.
158. Robison C, Krebs I, Binder S, Barbazetto IA, Kostolis AI, Yannuzzi LA, et al. Vitreo-macular adhesion in active and end-stage age-related macular degeneration. Am J Ophthalmol. 2009;148:79–82.
159. Russell SR. What we know (and do not know) about vitreoretinal adhesion. Retina. 2012;32:S181–6.